HHS Public Access

Author manuscript

Brain Behav Immun. Author manuscript; available in PMC 2020 August 01.

Published in final edited form as:

Brain Behav Immun. 2019 August ; 80: 73–87. doi:10.1016/j.bbi.2019.02.024.

Inhibition of NOX2 signaling limits pain-related behavior and improves motor function in male mice after spinal cord injury: participation of IL-10/miR-155 pathways

Boris Sabirzhanov[a,1], **Yun Li**[a,1], **Marino Coll-Miro**[a], **Jessica J. Matyas**[a], **Junyun He**[a], **Alok Kumar**[a,2], **Nicole Ward**[a], **Jingwen Yu**[a], **Alan I. Faden**[a,b,c], **Junfang Wu**[a,b,c,*]

[a]Department of Anesthesiology and Center for Shock, Trauma and Anesthesiology Research (STAR), University of Maryland School of Medicine, Baltimore, MD, 21201 USA.

[b]Department of Anatomy and Neurobiology, University of Maryland School of Medicine, Baltimore, MD, 21201 USA

[c]University of Maryland Center to Advance Chronic Pain Research, University of Maryland, Baltimore, MD, 21201 USA

Abstract

NADPH oxidase (NOX2) is an enzyme that induces reactive oxygen species (ROS) and serves as a switch between the pro-inflammatory and neurorestorative microglial/macrophage phenotypes; such changes play an important role in neuropathic pain and motor dysfunction. Increased NOX2 expression after spinal cord injury (SCI) has been reported, and inhibition of NOX2 improves motor function. However, the underlying mechanisms of NOX2 in post-traumatic pain and motor deficit remain unexplored. In the present study, we report that depletion of NOX2 ($NOX2^{-/-}$) or inhibition of NOX2 using NOX2ds-tat significantly reduced mechanical/thermal cutaneous hypersensitivity and motor dysfunction after moderate contusion SCI at T10 in male mice. Western blot (WB, 3 mm lesion area) and immunohistochemistry (IHC) showed that SCI elevates NOX2 expression predominantly in microglia/macrophages up to 8 weeks post-injury. Deletion of NOX2 significantly reduced $CD11b^{+}/CD45^{hi}F4/80^{+}$ macrophage infiltration at 24h post-injury detected by flow cytometry and $8\text{-}OHG^{+}$ ROS production at 8 weeks post-injury by IHC in both lesion area and lumbar enlargement. NOX2 deficiency also altered microglial/macrophage pro-inflammatory and anti-inflammatory balance towards the neurorestorative response. WB analysis

*Correspondence to Dr. Junfang Wu, University of Maryland School of Medicine, 655 W. Baltimore Street, Bressler Research Building, Room 6-009, Baltimore, MD 21201 USA; Tel: +1 410 706 5189; Fax: +1 410 706 1751. junfang.wu@som.umaryland.edu.

[2]Current address for A.K.: Department of Molecular Medicine and Biotechnology, Sanjay Gandhi Postgraduate Institute of Medical Sciences (SGPGIMS), Lucknow-226024, U.P., India.

[1]B.S. and Y.L. contributed equally to this work.

Authors' contributions

Author Contributions: JW conceived and designed research, with input from AIF; SB, YL, MCM, JJM, JH, AK, NW, JY, and JW performed research and analyzed data; JW wrote the manuscript with input from SB, YL, and AIF. All authors read and approved the final manuscript.

Conflict of interest statement

The authors have no conflicts of interest to declare.

showed robust increase of Arginase-1 and YM1 proteins in NOX2$^{-/-}$ mice. Furthermore, qPCR analysis showed significant up-regulation of anti-inflammatory cytokine IL-10 levels in NOX2$^{-/-}$ mice, associated with reduced microRNA-155 expression. These findings were confirmed in CD11b^{+} microglia/macrophages isolated from spinal cord at 3 days post-injury. Taken together, our data suggest an important role for IL-10/miR-155 pathway in regulating NOX2-mediated SCI-dysfunction. Thus, specific targeting of NOX2 may provide an effective strategy for treating neurological dysfunction in SCI patients.

Keywords

Spinal cord injury; NOX2 knock out; NOX2ds-tat; IL-10; miR-155; microglial/macrophage; pain-related behavior; motor function

1. Introduction

Spinal cord injury (SCI) results not only in sensorimotor deficits and autonomic changes, but also in a chronic, severe and often unrelenting pain that occurs in as many as 85% of SCI patients (Siddall et al., 2003; Stormer et al., 1997). Unfortunately, no known treatments consistently improve motor function or pain. This may reflect, in part, an incomplete understanding of complex secondary mechanisms. Activation of microglia/macrophages and associated neuroinflammation after SCI has been implicated as a mechanism for subsequent neurological dysfunction. However, no accepted current treatments specifically target neuroinflammatory mechanisms.

Accumulating evidence indicates that reactive oxygen species (ROS) contribute to the development of pain hypersensitivity (Little et al., 2012; Salvemini et al., 2011). ROS can act as specific signaling molecules in pain processing. Reduction of ROS levels by administration of scavengers or antioxidant compounds can attenuate the nociceptive behavior in various animal models of chronic pain (Gao et al., 2007; Kim et al., 2004; Lu et al., 2011; Siniscalco et al., 2007). Recent evidence shows that ROS may contribute to neuropathic pain in SCI animal models (Hulsebosch et al., 2009; Walters, 2014). Remarkably, NADPH oxidase (NOX2) is a critical inducer of both extracellular and intracellular ROS in microglia/macrophages (Lambeth, 2004); such inflammatory related changes play an important role in chronic neuropathic pain associated with a variety of conditions: peripheral neuropathy, visceral pain, capsaicin-induced hyperalgesia, and SCI-Pain (Hulsebosch et al., 2009; Kim et al., 2004). NOX2-related ROS expression in spinal cord microglia/macrophages has been implicated in neuropathic pain following peripheral nerve injury (Kallenborn-Gerhardt et al., 2014; Kim et al., 2010). In a rat model of chronic SCI-induced neuropathic pain, apocynin (a non-specific NADPH oxidase inhibitor) significantly reduced abnormal mechanical hypersensitivity, likely by inhibition of ROS (Hassler et al., 2014).

We and others have shown the importance of phagocytic NOX2 in microglial/macrophages activation and correlated production of pro-inflammatory factors after central nervous system (CNS) trauma (Cooney et al., 2014; Khayrullina et al., 2015; Kumar et al., 2016; Loane et al., 2014; Loane et al., 2013; Loane et al., 2009). Inhibition of NOX2 by NOX2ds-

tat (a peptide that specific inhibits NOX2) or NOX2 deletion by using NOX2 knockout ($NOX2^{-/-}$) mice are neuroprotective after ischemia/reperfusion injury and TBI (Chen et al., 2011; Chen et al., 2009; Kumar et al., 2016; Loane et al., 2013; Zhang et al., 2012). Increased NOX2 expression after SCI has been demonstrated in reactive microglia/macrophages surrounding the lesion for weeks after injury (von Leden et al., 2016). In a mouse SCI model, the combined use of the NOX2 inhibitor apocynin and the AMPA receptor inhibitor NBQX reduced lesion volume, increased preservation of white matter and a improved functional recovery up to 6 weeks post-injury (Johnstone et al., 2013). Acute inhibition of NOX2 by intrathecal single injection of NOX2ds-tat reduce long-term changes in motor function and microglial activity after SCI (Khayrullina et al., 2015). However, no studies to date have been examined effects of SCI using a $NOX2^{-/-}$ mouse model. Furthermore, the underlying mechanisms that regulate NOX2-dependent phenotypic changes in microglia/macrophages after SCI remain to be elucidated.

Because NOX2 protein is elevated in the spinal dorsal horn microglia after peripheral nerve injury and genetic deletion of NOX2 attenuates spinal nerve transection-induced mechanical and thermal hyperalgesia (Kim et al., 2010), the aims of the present study were to: (1) test whether genetic deletion or pharmacological inhibition of NOX2 limits SCI-induced cutaneous hypersensitivity and motor dysfunction; and (2) investigate the cell signaling mechanisms that regulate NOX2-mediated neurological dysfunction following SCI.

2. Materials and methods

2.1. Animals, spinal cord injury, and drug treatment

All experiments were conducted using either adult male C57BL/6 mice (20–25 g, purchased from Taconic, Rensselaer, NY), NOX2 knockout ($NOX2^{-/-}$; B6.129S-Cybbtm1Din/J, stock 002365; Jackson Laboratories, Bar Harbor, ME), or their age-matched C57BL/6 (WT) male mice. All animals were housed on a 12:12 h light/dark cycle with food and water available ad libitum. All procedures were carried out in accordance with protocols approved by the Institutional Animal Care and Use Committee (IACUC) at the University of Maryland School of Medicine.

A spinal cord contusion injury was produced using the Infinite Horizon (Precision Systems and Instrumentation) spinal cord impactor as previously described (Matyas et al., 2017; Wu et al., 2013; Wu et al., 2016a; Wu et al., 2014). Briefly, mice were deeply anesthetized with isoflurane evaporated in a gas mixture containing 70% N2O and 30% O2 and administered through a nose mask. The spinal column was stabilized using lateral clamps over the lateral processes at T9 and T11. A laminectomy was performed at T10 followed by a midline spinal impact with a force of 60 kilodyne for 2 sec dwell time, a moderate injury. Sham mice received laminectomy without contusion. Bladders of injured mice were manually expressed 2–3 times per day until a reflex bladder was established. All mice from both genotypes were randomly assigned to experimental groups and individuals involved in data analysis were blinded to group designations throughout all stages of the experiment. The number of mice at various time points in each study is indicated in the figure legends.

A potent selective NOX2 inhibitor, NOX2ds-tat (AnaSpec Inc. Fremont, CA) was completely dissolved in sterile saline and administered intraperitoneally (IP) once daily beginning 3 h post-injury and continuing for 7 days. Groups of mice received 5 mg/kg NOX2ds-tat or the equivalent volume of ds-tat scrambled peptide as a vehicle. This dose was based on reported therapeutic effects in mice (Abais et al., 2013). After SCI, mice were assigned to a treatment group according to a randomized block experimental design.

2.2. BMS for hind limbs locomotion

Mice were tested for hind limbs motor function in open field chamber on day 1 and days 3 after SCI and weekly thereafter for up to 6 weeks using the Basso Mouse Scale (BMS) by two investigators blinded to the genotype or treatment groups (Basso et al., 2006; Matyas et al., 2017; Wu et al., 2016a).

2.3. Mechanical and thermal allodynia tests

The development of mechanical allodynia after SCI was assessed using the Von Frey filament method as described previously (Wu et al., 2013; Wu et al., 2016b) by investigators blinded to the genotype or treatment groups. Briefly, each mouse was placed in individual Plexiglass chamber (model 37000–003, Ugo Basile SRL, Varese, Italy) on a wire mesh platform for 1 h to acclimate followed by testing. A series of von Frey filaments (Touch Test Sensory Evaluator Kit, Stoelting, #58011) with incremental stiffness ranging from 0.04 g to 2.0 g were applied to the plantar surface of each hind paw, beginning with the 0.04 g filament, until the fiber just bent, and held in place for 5 s or until a withdrawal response occurred. A valid response is defined as a brisk, complete withdrawal of the hind paw from the platform. Threshold was defined as the filament with the lowest bending force (at least 3 times out of 5 applications) (Matyas et al., 2017; Ren and Dubner, 1999; Wu et al., 2013).

An incremental hot plate (PE34; IITC Life Sciences, Woodland Hills, CA) was used to assess the thermal allodynia (Matyas et al., 2017; Wu et al., 2015; Wu et al., 2016b). Briefly, each mouse was allowed for 30 min for acclimation in a Plexiglass cylinder on the 30°C metal plate. The temperature of the plate at the time when the licking occurred was recorded as the outcome measure. Automatic cut-off temperature of 50°C was used to avoid tissue injury.

2.4. Western blot analysis

Mouse spinal cord tissues (approximately 3 mm) centered on the injury site were collected at indicated time and homogenized in RIPA buffer (Sigma-Aldrich) supplemented 1x protease inhibitor cocktail (Sigma-Aldrich), phosphatase inhibitor cocktail II and III (Sigma-Aldrich), sonicated and centrifuged at 20,000g for 20 min (Wu et al., 2015; Wu et al., 2016b). Protein concentrations were determined by the Pierce BCA method (ThermoFisher Scientific, US). Samples were run on 4–20% SDS-PAGE (Bio-Rad, Hercules, CA), and transferred to nitrocellulose membrane (Bio-Rad). Primary antibodies included: mouse anti-gp91^{phox} (NOX2; 1:500, Cat# 611415, BD Biosciences, San Diego, CA); mouse anti-arginase 1 (N-20) (1:1000; Cat# 610709, BD Transduction Laboratories, San Jose, CA), rabbit anti-Ym1 (1:1000; Cat# 60130, Stem Cell Technologies, Vancouver, BC, Canada), and mouse anti-Glyceraldehyde 3-phosphate dehydrogenase (GAPDH, 1:2000; Cat#

AB2302, Millipore, Temecula, CA). After incubation with the appropriate HRP conjugated secondary antibodies (KPL, Inc., Gaithersburg, MD), immune complexes were visualized using SuperSignal West Dura Extended Duration Substrate (Thermo Scientific, Rockford, IL). Chemiluminescence was imaged with a Kodak Image Station 4000R station (Carestream Health Inc., Rochester, NY) and protein bands were quantified by densitometric analysis using Carestream Molecular Imaging Software (Carestream Health Inc., Rochester, NY). The data presented reflects the intensity of a target protein band normalized by GAPDH and compared to sham for each sample (expressed in the fold of sham).

2.5. Immunohistochemistry and quantitative image analysis

Mice were intracardially perfused with saline, then with 4% paraformaldehyde at indicated time. After post-fixation and cryoprotection, the dissected 0.6-cm segment of spinal cord centered at the injury epicenter (lesion area) or 0.2-cm segment of lumber enlargement (L4–5) were coronally sectioned at 20μm thickness and thaw-mounted onto Superfrost Plus slides (ThermoFisher). Luxol fast blue (LFB) staining was used to determine the location of the injury epicenter with the least amount of spared white matter (Wu et al., 2012). SWM area was calculated at the injury epicenter as well as at points rostral and caudal to the epicenter by quantifying the total area stained by LFB. Images were taken at 2.5x magnification and analyzed using NIH ImageJ software. The threshold level of each 8-bit image was set to display only LFB-positive pixels, and total LFB-positive area was calculated for each section.

Coronal spinal cord sections were applied for immunohistochemistry (IHC) staining followed procedures described previously (Wu et al., 2013). The following primary antibodies were used: mouse anti-gp91^{phox} (NOX2; 1:500, Cat# 611415, BD Biosciences); rabbit anti-Ionized calcium binding adaptor molecule 1 (Iba-1, 1:1000, Cat# 019–19741, Wako Chemicals); mouse anti-NeuN (RBFOX3, 1:500, Cat# MAB377, Millipore), and mouse anti-8-hydroxyguanine (8-OHG, 1:200, Cat# ab10802, Abcam, Burlingame, CA). All immunohistological staining experiments were performed with appropriate positive control tissue as well as primary/secondary-only negative controls. For quantitative image analysis, images were acquired using a fluorescent Nikon Ti-E inverted microscope, at 20X (CFI Plan APO VC 20X NA 0.75 WD 1mm) magnification and the background of each image was subtracted using background ROI (Liu et al., 2015; Matyas et al., 2017). All images were quantified using Elements: nuclei were identified using Spot Detection algorithm; cells positive for any of the immunofluorescence markers were identified using Detect Regional Maxima algorithm, followed by global thresholding. The number of positive cells was normalized to the total imaged area (mm^2). For each experiment data from all images from one region in each mouse was summed up and used for final statistical analysis. At least 500–1000 cells were quantified per mouse per experiment. The number of NeuN labeled cells in the grey matter (GM) at the 0.6 mm rostral or caudal to the center was determined for each animal (2–4 images per location from 4–5 sections per mouse) from both sides of ventral/dorsal horns and intermediate GM. For NOX2/Iba-1 and 8-OHG/Iba-1, images were acquired 0.4 mm rostral or cordal to the epicenter or L4–5 spinal dorsal horns (LSDH), with n=2–4 images per location (whiter matter and grey matter) from four to five sections per mouse.

2.6. Isolation of CD11b+ microglia/macrophages

A magnetic-bead conjugated anti-CD11b antibody was used to isolate microglia/macrophages from spinal cord tissue of WT and NOX2$^{-/-}$ mice using MACS Separation technology (Miltenyi Biotec, Auburn, CA) as previously described (Holt and Olsen, 2016; Wu et al., 2010). Briefly, after intracardially perfusion with saline spinal cord tissue were rapidly dissected and dissociated by combining an optimized enzymatic treatment (Adult Brain Dissociation Kit; 130-107-677, Miltenyi Biotec) with gentle mechanical dissociation using the gentleMACS Octo Dissociator with Heaters (130-096-427, Miltenyi Biotec). Myelin was removed using Myelin Removal Beads II (130-096-733, Miltenyi Biotec) and LS columns (130-042-401, Miltenyi Biotec), and cell suspension were incubated with CD11b microbeads (130-093-634, Miltenyi Biotec) and loaded onto a MS column (130-096-335, Miltenyi Biotec) placed in the magnetic field of a MACS separator. The negative fraction (flow through) was collected, and the column was washed three times with MACS buffer. CD11b-positive cells were eluted by removing the magnetic field, resulting in the isolation of approximately 95% viable CD11b-positve cells from sham and SCI mice (data not shown).

2.7. Flow cytometry analysis

CD11b-selected cells were stained using anti-CD45-FITC (1:10, Cat#130-102-457, Miltenyi Biotech) and anti-F4/80-APC (1:50; Cat#17–4801-82, Life technology), or anti-CD11b-APC-efluor 780 (1:480, Cat# 47-0112-82, Invitrogen), anti-CD45-Efluor 450 (1:120, Cat# 48-0451-82, Invitrogen), and anti-F4/80-Alexa Fluor 647 (1:100; Cat# MF48021, Invitrogen) for 30 min at 4°C in the dark. Cells were washed twice with 1 ml of FACS buffer, fixed using 1% paraformaldehyde, and 20,000 events were recorded using a BD FACS Canto II cytometer (BD Bioscience). Gating was determined based on appropriate negative isotype controls. Infiltrating macrophage and microglia was determined by gating on CD11b+CD45^{hi}F4/80+ (infiltrating macrophages) and CD11b+CD45^{int} (microglia) cells (Kumar et al., 2015). Data was analyzed using FlowJo Software (v.X; TreeStar, Inc., Ashland, OR).

2.8. Quantitative PCR (qPCR) analysis

Total RNA was isolated using miRNeasy Kit (Qiagen) with on-column DNase treatment (Qiagen, Valencia, CA). cDNA synthesis was performed on 1 μg of total RNA using a Verso cDNA RT kit (Thermo Scientific, Pittsburg, PA); according to the manufacturer'sprotocol. qPCR amplification was performed by using cDNA TaqMan Universal Master Mix II (Applied Biosystems). Gene expression assays for the following genes were used: TNFα (Mm00443258_m1), IL-1β (Mm0133–6189_m1), inducible nitric oxide synthase (iNOS; Mm00440502_m1), IL-6 (Mm00446190_m1), formyl peptide receptor 2 (Fpr2; Mm01157717_s1), Arginase 1 (Arg-1, Mm00475988_m1), chitinase-like protein 3 (Ym1, also called Chil3, Mm00657889_mH), IL-4Rα (Mm012751 39_m1), suppressor of cytokine signalling 3 (SOCS3, Mm00545913_s1), SOCS1 (Mm01342740_g1), NOX4 (Mm00479246_m1), and IL-10 (Mm0–0439614_m1). Gene expression was normalized to GAPDH (Mm99999915_g1) and the relative quantity of mRNAs was calculated based on the comparative Ct method (Wu et al., 2015; Wu et al., 2014).

We used qPCR to measure the expression of mmu-miR-155–5p. 10 ng of total RNA was reverse transcribed using TaqMan miRNA Reverse Transcription Kit (Applied Biosystems) with miRNA-specific primers. Reverse transcription reaction products (1.5 μl) were used for qPCR. Following TaqMan miR Expression assays were used: mmu-miR-155–5p (002571) and U6 snRNA (001973) (Applied Biosystems). qRT-PCR amplification was performed by using cDNA TaqMan Universal Master Mix II (Applied Biosystems). Reactions were amplified and quantified using a 7900HT Fast Real-Time PCR System and the corresponding software (Applied Biosystems). miR-155–5p expression was normalized to U6 snRNA, and the relative quantity of miR-155–5p was calculated based on the comparative Ct method (Sabirzhanov et al., 2016; Sabirzhanov et al., 2014).

2.9. Statistical analysis

All data as shown represent the mean±SEM. All statistical analyses were conducted by using the GraphPad Prism Program, Version 3.02 for Windows (GraphPad Software; RRID:SCR_002798) or SigmaPlot, version 12 (Systat Software; RRID:SCR_003210). BMS and allodynia tests were analyzed using two-way ANOVA with repeated measures followed by Student's Newman–Keuls post hoc test. For multiple comparisons, one-way ANOVA was performed followed by Student's Newman–Keuls post hoc test for parametric (normality and equal variance passed) data. A p value of <0.05 was considered statistically significant.

3. Results

3.1. SCI induces NOX2 expression predominantly in microglial/macrophages

To evaluate the effect of SCI on NOX2 dysregulation, we examined level of NOX2 protein from 6 h to 28 d after contusion injury. Quantitative analysis of western blots (one-way ANOVA followed by Newman–Keuls post hoc test, $F(5,17)=52.74$, $p<0.0001$) showed that the expression of NOX2 was rapidly upregulated within 24 h (15 to 20 fold, $p<0.001$) in injured spinal cord tissue (n=3–5 mice/time-point) compared with sham tissue (n=6), remaining elevated for at least 14 days after SCI ($p<0.05$, Fig. 1A–B).

The level of NOX2 was also examined at the lesion site by IHC. In the intact spinal cord, NOX2 positive cells were barely detected (data not shown). At 24h after SCI, the up-regulation of NOX2 in the spinal cord was predominantly found in Iba-1^+ microglia/macrophagy (Fig. 1C). Previous reports (Bermudez et al., 2016; Byrnes et al., 2011; Loane et al., 2014) indicate that NOX2 expression in microglia/macrophagy assessed by IHC remains upregulated for months after CNS injury. We assumed that chronic elevation of NOX2 after SCI may contribute to long-term neurological dysfunction. IHC analysis showed that $NOX2^+$/Iba-1^+ cells remained significant increase (3 fold) up to 8 weeks post-injury (n=5, two-tailed unpaired t-test, $p<0.01$, $F(4,4)=2.4$, Fig. 1D–E).

3.2. Genetic deletion or pharmacological inhibition of NOX2 limits SCI-induced hyperesthesia and motor dysfunction

To test whether changes in NOX2 regulation are associated with nocifensive responses or locomotor recovery after SCI, elimination of NOX2 gene in $NOX2^{-/-}$ mice were assessed weekly for locomotor function and mechanical/thermal hyperesthesia. Hindlimb locomotor

function was assessed using the BMS. By day 7, the NOX2$^{-/-}$ mice (n=9) showed significantly higher BMS scores than the WT mice (n=9, Fig. 2A; $p<0.01$), which persisted through 42 d. The factor of Postinjury Days ($F(9,288)=84.967$; $p<0.001$) in BMS test was found to be significant. The factor of Genotypes ($F(3,288)=121.496$; $p<0.001$) as well as the interaction of Postinjury Days × Genotypes ($F(27,288)=29.823$; $p<0.001$; repeated measures two-way ANOVA) were also significant. To quantify improvements in the areas of stepping frequency, coordination, paw position, trunk stability, and tail position, the BMS subscore was evaluated. NOX2$^{-/-}$ mice demonstrated a recovery in more fine motor control, as shown in the BMS subscore (Fig. 2B), with significant improvement at 14 d, which remained through 42 d after injury. The factors of Postinjury Days ($F(7,128)=19.736$; $p<0.001$), Genotypes ($F(1,128)=47.676$; $p<0.001$), and the interaction of Postinjury Days × Genotypes ($F(7,128)=3.829$; $p<0.001$; repeated measures two way ANOVA) were found to be significant. Therefore, mice lacking NOX2 have better functional recovery after SCI than the WT mice.

Nocifensive behaviors were tested before the injury and at 27, 34, and 55 days post-injury when mice regained adequate locomotor function to be able to withdraw a hindpaw from a stimulus. No difference in mechanical threshold or response to thermal (hot) stimuli was found between the genotypes before SCI. On days 27–28 after SCI, the NOX2$^{-/-}$ mice (n=14) had a significantly higher mechanical/hot threshold than the WT mice (n=13), indicating less cutaneous hypersensitivity, and these differences persisted to days 55–56 ($p<0.01$, two-way ANOVA with repeated measures followed by Student's Newman–Keuls post hoc analysis, Fig. 2C–D). Two way ANOVA analysis in the von Frey filament test showed significant effects of Postinjury ($F(3,81)=55.30$; $p<0.001$) and Genotypes ($F(1,81)=18.919$; $p<0.001$). The interaction of Postinjury × Genotypes ($F(3,81)=1.786$; $p=0.156$) was not significant. In the thermal hyperalgesia test, the factors of Postinjury Days ($F(3,73)=22.531$; $p<0.001$) and Genotypes ($F(1,73)=19.254$; $p<0.001$) were found to be significant. However, the interaction of Postinjury Days × Genotypes ($F(3,73)=2.710$; $p=0.051$) was not significant.

To examine the effect of inhibiting NOX2 on locomotor functional recovery in mice contusion model, the C57BL/6 mice subjected to a moderate contusion SCI or sham received an ip injection of NOX2ds-tat (5 mg/kg), a potent selective NOX2 inhibitor or vehicle beginning at 3 hours post-injury and once daily for 7 days. By 1 week after injury, NOX2ds-tat-treated mice (n=12) had significantly improved BMS scores compared with ds-tat scrambled peptide (vehicle)-treated animals (n=13, $p<0.001$), which remained through 6 weeks after injury (Fig. 2E). The factor of Postinjury Days ($F(7,322)=139.502$; $p<0.001$) in BMS test was found to be significant. The factor of Drug ($F(3,322)=271.846$; $p<0.001$) as well as the interaction of Postinjury Days × Drug ($F(21,322)=49.321$; $p<0.001$; repeated measures two-way ANOVA) were also significant. Furthermore, NOX2ds-tat-treated mice demonstrated an improvement in the fine details of locomotion, as shown in the BMS subscore (Fig. 2F), with a significant recovery at 21 d, which persisted through 42 d after injury. The factors of Postinjury Days ($F(7,184)=13.163$; $p<0.001$), Drug ($F(1,184)=34.469$; $p<0.001$), and the interaction of Postinjury Days × Drug ($F(7,184)=3.732$; $p<0.001$; repeated measures two-way ANOVA) were found to be significant.

There was no difference in mechanical/thermal threshold between the groups before the SCI. On days 27–28 after SCI, NOX2ds-tat-treated mice (n=9) had a significantly higher mechanical threshold than the vehicle treated mice (n=7, $p<0.001$), indicating less mechanical cutaneous hypersensitivity, and these differences persisted to days 55–56 ($p<0.01$, Fig. 2G). The threshold for hot plate temperature was decreased in the vehicle group, whereas NOX2ds-tat reversed the hot threshold to the basal level ($p<0.001$, Fig. 2H). Two way ANOVA analysis in the von Frey filament test showed significant effects of Postinjury ($F(3,42)=66.136$; $p<0.001$), Drug ($F(1,42)=10.164$; $p=0.007$), and the interaction of Postinjury × Drug ($F(3,42)=5.930$; $p=0.002$). In the thermal stimulation test, the factors of Postinjury Days ($F(3,42)=32.053$; $p<0.001$), Drug ($F(1,42)=16.974$; $p=0.001$), and the interaction of Postinjury Days × Drug ($F(3,42)=3.233$; $p=0.032$) were found to be significant.

3.3. Depletion of NOX2 increases the spared white matter area and surviving neurons at 8 weeks after SCI

To determine if the observed behavioral improvement may relate to increased amount of spared WM, spinal cord sections from injured mice perfused at 8 weeks after SCI were stained with LFB and the WM area was quantified at 200 μm intervals rostral and caudal to the injury epicenter (EPI). Animals with NOX2 gene deletion showed significantly increased WM sparing (two-tailed unpaired t-test between two groups, $F(10,10)=1.886$, $p<0.0001$). Further multiple t tests indicated significantly differences of SWM at rostral and caudal to the epicenter between two groups (Fig. 3A–B). Representative LFB-stained sections illustrate the differences in SWM area between the $NOX2^{-/-}$ mice and the WT mice.

Surviving neurons were also examined at 8 weeks after SCI (Fig. 3C–D). SCI resulted in 39% of neuronal cell loss (41.5 ± 2.6 vs. 67.5 ± 2.2 $NeuN^+$ cells for SCI/WT and Sham/WT samples, respectively. $p<0.01$), whereas depletion of NOX2 significantly improved neuronal survival at 8 weeks after injury when compared with SCI/WT samples (Fig. 3C, 57.6 ± 2.4 vs. 41.5 ± 2.6 $NeuN^+$ cells for SCI/$NOX2^{-/-}$ and SCI/WT samples, respectively. $p<0.05$). The factor of Genotypes [$F(3,20)=5.853$, $p=0.0049$; one-way ANOVA followed by Newman–Keuls post hoc test] was found to be significant. There was no difference in $NeuN^+$ cells between Sham/WT and Sham/$NOX2^{-/-}$ groups.

3.4. Deletion of NOX2 reduces macrophage infiltration and ROS production after SCI

After mid-thoracic SCI, rapid microglial hypertrophy and cytokine production are found spreading well-below the injury, such as the lumbar enlargement (L4–5) where is directly associated with hind-paw neuropathic pain (Detloff et al., 2008; Gwak et al., 2012; Peng et al., 2006). Macrophages from the periphery and activated microglia appear in the spinal cord between 12 and 24 hours after injury (Loane and Byrnes, 2010). Moreover, depletion of NOX2 in mouse brain injury model robustly reduces pro-inflammatory signaling at 24 h post-injury (Kumar et al., 2015; Kumar et al., 2016). Based on our pilot data, at 24h post-injury, we then addressed whether the observed behavioral improvements in $NOX2^{-/-}$ mice related to the changes of microglia and macrophage infiltration at the lesion site and lumbar spinal cord. Flow cytometry was performed in isolated $CD11b^+$ cells. When compared to sham control levels (Sham/WT, n=5), SCI significantly increased the number of CD11b

$^{+}$CD45^{hi}/F4/80^{+} cells at lesion area at 24h post-injury (SCI/WT, n=6, p<0.01; Fig. 4A–B). Deleting NOX2 reduced infiltrating macrophages by approximately 50% (SCI/KO, n=5, p<0.05). The factor of Genotypes (F(3,17)=14.03; p<0.0001; one-way ANOVA followed by Newman–Keuls post hoc test) was found to be significant. There was no genotype effect on CD11b^{+}/CD45^{hi}/F4/80^{+} cells in Sham groups. Remarkably, these cells at the L4–5 were also significantly reduced in NOX2$^{-/-}$ mice (n=6, p<0.001, Fig. 4C), indicating that reduced numbers of macrophages infiltrated the lumber spinal cord in NOX2$^{-/-}$ SCI mice. The factor of Genotypes (F(3,20)=12.48; p<0.0001; one-way ANOVA followed by Newman–Keuls post hoc test) was found to be significant. However, CD11b^{+}/CD45^{int} populations were found no significant difference in both lesion area (Sham/WT: 37.4±12.4; Sham/KO: 45.7±12.9; SCI/WT: 59.6±11.5; SCI/KO 47.1±12.5; n=6/group) and lumbar 4/5 cord (Sham/WT: 34.2±9.9; Sham/KO: 45.8±10.1; SCI/WT: 47.1±14.4; SCI/KO 40.5±12.8; n=6/group) from WT and NOX2−/− (KO) sham and SCI mice at 1d post-injury. The factors of Genotypes [Lesion area: F(3,20)=0.5532; p=0.6519; Lumber cord: F(3,20)=0.2445; p=0.8642; one-way ANOVA followed by Newman–Keuls post hoc test] were not significant.

Chronic elevation of ROS after SCI may contribute to long-term neurological dysfunction including pain maintenance. Thus, IHC was performed at 8 weeks post-injury after completion of behavioral tests. The ROS production at both lesion area and the lumbar 4–5 spinal cord dorsal horns (LSDH) was assessed by IHC using 8-hydroxyguanine (8-OHG) antibody (Bermudez et al., 2016; Kim et al., 2010) that detects oxidized nucleic acid, which results from cellular ROS damage. Eight weeks after SCI, 8-OHG^{+} cells in Iba-1^{+} microglia/macrophage population were significantly increased at the lesion area [one-way ANOVA followed by Newman–Keuls post hoc test, F(3,22)=19.08, p<0.0001] as well as LSDH (F(3,23)=21.80, p<0.0001, n=8 mice in WT/SCI group) compared to Sham mice (n=7 mice in Sham/WT group, Fig. 5A–B). The number of 8-OHG^{+}/Iba-1^{+} cells significantly reduced in the NOX2−/− mice (n=5 mice in SCI/NOX2 KO group, p<0.01) compared to WT/SCI group, indicating reduced production of ROS. Some of the 8-OHG^{+} cells in the grey matter were Iba-1- (arrowheads) from SCI mice (Fig. C).

3.5. NOX2 depletion attenuates M1-like activation and promotes M2-like activation

NOX2 is thought to regulate polarization mechanisms in microglia/macrophage (Choi et al., 2012; Kumar et al., 2016). After CNS trauma, pro-inflammatory mediators peak at 24h post-injury (Kumar et al., 2015; Loane and Byrnes, 2010). To test whether NOX2 drives a neurotoxic M1-like neuroinflammatory response after SCI, we collected spinal cord tissue (approximately 3 mm centered on the injury site) at 1 day post-injury to assess gene expression profiles for selected M1-like activation markers. TNFα, IL-1β, and iNOS are pro-inflammatory markers that can be produced by M1-polarized microglia/macrophages (Kigerl et al., 2009). The IL-6 is the major pro-inflammatory cytokine produced by various cells including activated microglia/macrophages (Wu et al., 2014). Fpr2 is G-protein coupled receptor highly expressed in M1-polarized microglia/macrophages (Jablonski et al., 2015). SCI significantly increased mRNA levels of TNFα, IL-1β, iNOS, IL-6, and Fpr2 in WT mice when compared with levels in sham controls (n=6, p < 0.001; Fig. 6A). In contrast, SCI in NOX2$^{-/-}$ mice resulted in a significant reduction of all M1-likegenes mRNAs (n=7, p < 0.05 [TNFα, IL-6, IL-1β, Fpr2], p < 0.001 [iNOS]), indicative of a reduced M1-like

response in NOX2$^{-/-}$ SCI mice when compared to WT SCI mice. The factors of Genotypes [F(3,18)=58.08; p<0.0001 for TNFα; F(3,20)=27.91; p<0.0001 for IL-1β; F(3,15)=15.41; p<0.0001 for iNOS; F(3,18)=16.86; p<0.0001 for IL-6; F(3,18)=13.18; p<0.0001 for Fpr2; one-way ANOVA followed by Newman–Keuls post hoc test] were found to be significant.

We next evaluated alternative or M2-like activation responses after SCI. Ym1 is an established marker of the IL-4–induced alternatively activated macrophage phenotype. Macrophage-specific Arg1 functions as an inhibitor of inflammation. IL-4Rα is an important modulator of IL-4 and IL-13 receptor binding. SOCS3 is involved in repressing the M1 proinflammatory phenotype, thereby deactivating inflammatory responses in macrophages (Qin et al., 2012) and M2 macrophage highly expresses upregulated SOCS3 (Zhou et al., 2017). *In vitro*, stimulation of macrophages with anti-inflammatory IL-10 leads to the upregulation of SOCS3 (Gordon, 2003). Depletion of NOX2 causes robustly elevated SOCS3 expression after TBI (Barrett et al., 2017). These genes are highly expressed by M2-polarized microglia/macrophages and robustly elevated after CNS injury (Kigerl et al., 2009; Kumar et al., 2015). mRNA analysis of M2-like markers revealed that SCI significantly increased levels of Arg1, SOCS3, and IL-4Rα expression in WT mice (n=5) when compared to levels in sham controls (n=5, p < 0.001, Fig. 6B. One-way ANOVA followed by Student's Newman–Keuls post hoc). Ym1 mRNA levels were also significantly elevated in the WT/SCI group compared to Sham mice analyzed by Mann Whitney test. Remarkably, SCI in NOX2$^{-/-}$ mice resulted in significantly increased expression levels of Ym1, Arg1, SOCS3, and IL-4Rα mRNA [p < 0.01 (Ym1), p < 0.05 (Arg1, IL-4Rα), and p < 0.001 (SOCS3)] when compared to levels in WT/SCI group. The factors of Genotypes [F(3,18)=12.63; p=0.0001 for Ym1; F(3,13)=32.66; p<0.0001 for Arg1; F(3,18)=78.82; p<0.0001 for SOCS3; F(3,18)=29.81; p<0.0001 for IL-4Rα; one-way ANOVA followed by Newman–Keuls post hoc test] were found to be significant.

As SOCS1 has been considered an anti-inflammatory "counterpart" to SOCS3, we also examined SCOS1 expression at 1 day post-injury. Surprisingly, SCI caused significantly decreased in SOCS1 expression in both WT (0.34±0.09, p<0.01) and NOX2$^{-/-}$ mice (0.55±0.12, p<0.05) compared to Sham/WT mice (1.06±0.16). The factor of Genotypes (F(3,20)=5.232; p=0.0079; one-way ANOVA followed by Newman–Keuls post hoc test) was significant. However, depletion of NOX2 (n=6) did not significantly alter SCOS1 expression compared to SCI/WT mice (n=6).

Although robust changes of Arg1 and Ym1 at mRNA levels, their protein levels by western blot were not detectable until 3 days post-injury. Based on prior work in TBI (Kumar et al., 2016) and our pilot data in SCI, we assessed Ym1 and Arg1 protein levels in injured spinal cord at 3 days post-injury. We observed significant increase in Ym1 and Arg1 level in NOX2$^{-/-}$ SCI mice (n=5) when compared to WT/SCI mice [n=5, p < 0.001 (Arg1), p<0.01 (Ym1); Fig. 6C–E). The factors of Genotypes [F(3,17)=27.39; p<0.0001 for Arg1; F(3,17)=17.40; p<0.0001 for Ym1; one-way ANOVA followed by Newman–Keuls post hoc test] were found to be significant. Taken together, these data demonstrate that NOX2 deficiency mitigates the M1-like response and promotes M2-like activation after SCI.

The NOX4 isoform is also an early initiator of neuropathic pain following SCI (Im et al., 2012). To determine if the observed reduced inflammatory response in NOX2$^{-/-}$ mice may relate to the decreased expression of NOX4, we examined NOX4 expression level at 1 day post-injury. mRNA analysis revealed that SCI significantly increased levels of NOX4 expression in WT mice (n=6) when compared to levels in sham controls (n=6, $p<0.01$, Fig. 6F). In contrast, SCI in NOX2$^{-/-}$ mice resulted in a significant reduction of NOX4 mRNA (n=6, $p<0.05$). The factor of Genotypes ($F(3,20)=6.179$; $p=0.0038$; one-way ANOVA followed by Newman–Keuls post hoc test) was found to be significant.

3.6. NOX2 deficiency alters IL-10/miR- 155 expression

IL-10 is a potent anti-inflammatory cytokine that is crucial for downregulation of pro-inflammatory genes which are induced by Toll-like Receptor (TLR) signaling. Prior works report (Barrett et al., 2017; Mukhamedshina et al., 2017) that CNS trauma increases IL-10 mRNA in the injured cortex or spinal cord during 1–7 days post-injury. Recently, IL-10 is found significantly increased in microglia/macrophages in the injured brain of NOX2$^{-/-}$ mice at 3–7 days (Barrett et al., 2017). Thus, we hypothesized that NOX2 deficiency alters post-injury microglia/macrophage phenotypes towards beneficial M2-like activation through enhanced IL-10 signaling. We then set out to evaluate genotype-related changes in IL-10 expression in the injured spinal cord tissue at first week post-injury. IL-10 mRNA expression was measured in lesion area of sham and SCI WT and NOX2$^{-/-}$ mice at 1, 3, and 7 days post-injury (Fig. 7A). IL-10 expression was significantly increased in WT and NOX2$^{-/-}$ SCI mice compared to sham levels (n=6 mice/group) at 3 and 7 days post-injury. The factors of Postinjury Days ($F(3,18)=10.53$; $p=0.0003$ in WT; $F(3,18)=21.74$; $p<0.0001$ in NOX2$^{-/-}$; one-way ANOVA followed by Newman–Keuls post hoc test) were found to be significant. Notably, there was a significant increase in IL-10 expression in NOX2$^{-/-}$ SCI mice at 3 and 7 days when compared to WT SCI mice [n=5/group; $p<0.01$ (3 days); $p<0.05$ (7 days), Mann Whitney two-tailed test].

After CNS trauma, proliferation and activation of CD11b^{+} microglia/macrophages peak between 3 and 7 days post-injury. Based on prior work in NOX2/TBI study (Barrett et al., 2017), CD11b cells were isolated from injured spinal cord tissues at 3 d post-injury. SCI significantly increased IL-10 expression in the CD11b^{+} cells derived from SCI WT mice compare to Sham/WT group (n=7 per group, $p<0.001$) (Fig. 7B). Notably, there was a significant increase in IL-10 expression in NOX2$^{-/-}$ SCI mice compare to WT/SCI mice (n=7 per group, $p<0.001$). The factor of Genotypes ($F(3,24)=110.2$; $p<0.0001$; one-way ANOVA followed by Newman–Keuls post hoc test) was found to be significant. Together, these data indicate that NOX2 deficiency results in a significant increase in IL-10 expression in microglia/macrophages during the acute-subacute phase following SCI.

miR-155 is known to critically regulates inflammatory signaling in neurological disorders (Gaudet et al., 2017) and depletion of miR-155 reduce inflammation and post-SCI tissue damage (Gaudet et al., 2016). After CNS trauma, miR-155 expression is elevated in the injured cortex or spinal cord at 1 and 7 days post-injury (Gaudet et al., 2016; Henry et al., 2018). Studies also show that increased IL-10 inhibits potent pro-inflammatory miR-155 induction in response to lipopolysaccharides (LPS) stimulation (McCoy et al., 2010). Thus,

we hypothesized that NOX2 deficiency reduces post-SCI neuroinflammation through elevated IL-10 signaling leading to downregulated miR155 induction. To investigate the potential role of NOX2 in the regulation of miR-155 level, we examined post-injury changes in miR-155 expression in injured spinal cord tissue (Fig. 8A). In agreement with the prior report (Gaudet et al., 2016), SCI in WT mice induced the rapid and robust increase of miR-155 expression at 1 and 3 days (4–5-fold higher than uninjured; n=5–6/group). miR-155 remained elevated at 7 days (5-fold; $p<0.001$, n=5). In the absence of NOX2, SCI also caused elevation of miR-155. The factors of Postinjury Days ($F(3,18)=11.54$; $p=0.0002$ in WT; $F(3,18)=6.012$; $p=0.0051$ in $NOX2^{-/-}$; one-way ANOVA followed by Newman–Keuls post hoc test) were found to be significant. Importantly, there was a significant reduction in miR-155 expression in $NOX2^{-/-}$ SCI mice (n=5–6/group) at all time-points selected when compared to WT/SCI mice [$p<0.05$ (d1, d3); $p<0.01$ (d7); Mann Whitney two-tailed test]. We also found reduced miR-155 expression in Sham/$NOX2^{-/-}$ mice compared to Sham/WT animals ($p<0.05$). Furthermore, miR-155 was upregulated in $CD11b^{+}$ cells isolated form injured spinal cord tissues at 3 days post-injury (4.5-fold higher than Sham/WT; $p<0.001$; Fig. 8B). Reduced miR-155 expression was confirmed in CD11b-selective microglia/macrophages in the absence of NOX2. The factor of Genotypes ($F(3,27)=105$; $p<0.0001$; one-way ANOVA followed by Newman–Keuls post hoc test) was found to be significant [N=9 (Sham/WT), 8 (Sham/$NOX2^{-/-}$), 7 (SCI/WT), and 7 (SCI/$NOX2^{-/-}$) mice/group]. Therefore, reduced post-SCI inflammation in $NOX2^{-/-}$ spinal cords is associated with significant up-regulation of IL-10 and downregulation of miR-155.

4. Discussion

In the present study, we show that systemic administration of the specific NOX2 inhibitor NOX2ds-tat or depletion of NOX2 attenuate the development of mechanical/thermal cutaneous hypersensitivity and improve locomotor function following thoracic spinal cord contusion in mice. $NOX2^{-/-}$ mice display reduced tissue damage and increased survival neurons after SCI. Depletion of NOX2 reduces infiltrating macrophages, ROS production, as well as expression levels of pro-inflammatory genes. Moreover, deleting NOX2 also enhances the expression of anti-inflammatory genes and decreases elevation of pro-inflammatory miR-155 in microglia/macrophages. Together, these data suggest an important role for IL-10/miR-155 pathway in regulating NOX2-mediated SCI-dysfunction.

Among NOX family members, NOX2 is the most responsive to injury (von Leden et al., 2016). Although increased $NOX2^{+}$ cells in injured spinal cord have been reported (Cooney et al., 2014), no studies to date have systemically examined NOX2 protein expression after SCI. NOX2 protein expression was robustly elevated as early as 6 h after SCI, after which expression declined, but remained elevated through 28 days post-injury over sham-injured tissue. Given large tissue total homogenate (3 mm centered on the injury site) and diluted signaling by western blot, we did not observe a significant difference in NOX2 protein level at 28 days post-injury. Consistent with previous reports (Bermudez et al., 2016; Byrnes et al., 2011; Loane et al., 2014) that NOX2 expression remains upregulated for months after CNS injury, using IHC, we show a significant increase of NOX2 in microglia/macrophages in the lesion area at 8 weeks post-injury.

In a mouse SCI model, central inhibition of NOX2 by a single intrathecal injection of NOX2ds-tat immediately after injury improved locomotor functional recovery (Khayrullina et al., 2015); however, this treatment paradigm did not reduce inflammation beyond 7 days. Furthermore, no studies to date have been performed in SCI using a NOX2 knockout mouse model. To investigate the effects of NOX2 on SCI-induced neurological dysfunction, systemic NOX2 inhibition by NOX2 ds-tat ip injection or transgenic $NOX2^{-/-}$ mice were applied. We found significant overall improvements in depletion or inhibition of NOX2 mice compared with control animals. These improvements were significant by 7 days post-injury and continued through 6 weeks. The NOX inhibitor apocynin has been shown to reduce SCI-pain (Hassler et al., 2014), but it non-specifically inhibits the entire NOX family. No studies to date have been performed in SCI-pain using a specific NOX2 inhibitor or $NOX2^{-/-}$ mice. We observed reduced mechanical/thermal cutaneous hypersensitivity in NOX2ds-tat-treated mice as compared to vehicle-treated animals, as well as in $NOX2^{-/-}$ mice as compared to their WT littermates. The degree of locomotor recovery after contusion SCI is highly correlative with tissue pathology (Basso et al., 2006). Increased white matter sparing and the number of survival neurons resulting from $NOX2^{-/-}$ mice were found both rostral and caudal to the lesion site, contributing to improved functional recovery. Thus, specific targeting of NOX2 enzyme may provide an effective strategy for treating chronic pain as well as motor dysfunction in SCI patients.

After SCI, both resident microglia and infiltrating peripheral immune cells, including macrophages, contribute to pro-inflammatory processes and tissue damage at the lesion epicenter (David and Kroner, 2011; Gensel and Zhang, 2015). Furthermore, inflammation spreads past the lesion area through the lumbar cord after a thoracic SCI (Gwak et al., 2012; Hansen et al., 2013). In addition, there is rapid pro-inflammatory macrophage infiltration (24 h) into the lumbar cord after mid-thoracic contusion (Norden et al., 2018; Schwab and Bartholdi, 1996; Vargas and Barres, 2007). This is important because inflammation in these segments not only impedes motor recovery but also mediates mechanical hypersensitivity (Detloff et al., 2008; Hansen et al., 2013; Hulsebosch, 2008; Peng et al., 2006). Thus, modulating inflammation within the lumbar microenvironment may provide an intervention to potentiate the recovery of locomotion and limit the development of neuropathic pain.

After CNS trauma, NOX2 is highly expressed by infiltrating macrophages that are highly inflammatory (Kumar et al., 2016; von Leden et al., 2016; Zhang et al., 2016). In the present study, flow cytometry reveals that NOX2 deletion decreases the accumulation of $CD11b^{+}$/$CD45^{hi}$/$F4/80^{+}$ macrophages by 51% (T10) and 24% (L4–5) when compared to WT SCI group, indicating robust reduction of macrophage infiltration in $NOX2^{-/-}$ mice. Recent studies (Barrett et al., 2017; Kim et al., 2010; Kumar et al., 2016) indicate that upregulation of NOX2 contributes to macrophages ROS-mediated damage in neurotrauma. After CNS injury, blood-brain barrier (BBB) permeability is increased up to weeks post-injury. NOX2 deficiency significantly reduces BBB disruption after focal cerebral ischemia (Liu et al., 2011). In experimental autoimmune encephalomyelitis (EAE) *in vitro* studies, NOX inhibition with apocynin reduces BBB permeability seen in EAE (Choi et al., 2015; Seo et al., 2016). After TBI (Kumar et al., 2016), $NOX2^{-/-}$ mice display reduced microglia/macrophage in the injured cortex. Thus, reduced accumulation of macrophage observed in the $NOX2^{-/-}$ SCI mice in the present study could be attributed to improved blood-spinal

cord barrier disruption. Whether or not NOX2 deficiency alters infiltrated macrophage proliferation after SCI is intriguing for further investigation. However, SCI-induced ROS production can derive from both activated macrophages and microglia (Fleming et al., 2006). Although no difference of $CD11b^{+}/CD45^{int}$ microglia in both lesion area and lumbar 4/5 cord from WT and $NOX2^{-/-}$ sham and SCI mice at 1d post-injury, NOX2 deficiency attenuates M1-like activation suggesting reduced activation of microglia/macrophages in $NOX2^{-/-}$ mice. Thus, reduced microglial activation and infiltrating macrophages observed in the present study likely contribute to the reduction of ROS production in $NOX2^{-/-}$ mice, leading to improved recovery. In addition, SCI causes pathological changes in dorsal root ganglia (DRG) (Chhaya et al., 2018; Ritter et al., 2015) where nociceptor cell bodies reside and play an important role in the peripheral mechanism of sensation by primary afferent neurons. NOX2-dependent ROS production in infiltrated macrophages at the DRG following SCI may contribute to pain development. If depletion or inhibition of NOX2 alters macrophages infiltration at DRG level is intriguing for future study.

We and others have shown the importance of phagocytic NOX2 in microglial/macrophages activation and correlated production of pro-inflammatory factors, along with chronic neuronal cell loss and associated neurological dysfunction after TBI or SCI (Cooney et al., 2014; Khayrullina et al., 2015; Kumar et al., 2016; Loane et al., 2014; Loane et al., 2013; Loane et al., 2009). Chronic and excessively M1-like activation in microglia can lead to exacerbation of injury and progressive tissue destruction, whereas the M2-like microglial activation serves to dampen the inflammatory response and promote tissue repair (Gordon, 2003; Lynch, 2009). Our data in a mouse SCI model indicate that increased NOX2 activity after SCI drives M1-like activation that contributes to inflammatory-mediated neurological dysfunction, and that NOX2 depletion results in enhanced expression of M2-anti-inflammatory markers. Thus, depletion of NOX2 provides neuroprotection, in part by altering M1-/M2-like balance towards the M2-like anti-neuroinflammatory response. SCI also causes NOX4 upregulation acutely in glial cells (Bermudez et al., 2016; Cooney et al., 2014; Im et al., 2012), which is known to play an important role in neuropathic pain (Im et al., 2012). Consistent with prior reports (Bermudez et al., 2016; Cooney et al., 2014; Im et al., 2012), we found elevated expression of NOX4 mRNA in both WT and $NOX2^{-/-}$ mice at 1 day post-injury. Depletion of NOX2 significantly reduces NOX4 mRNA level. Whether or not NOX4 needs NOX2 to function efficiently is intriguing for future investigation.

Reduced microglia and infiltrating macrophages are likely major contributors to the anti-inflammatory environment in the SCI tissue in $NOX2^{-/-}$ mice. However, the underlying mechanisms of NOX2 in the regulation of microglia/macrophages remain unclear. IL-10 is a potent anti-inflammatory cytokine and has been correlated with the downregulation of macrophage and microglial activity (Abraham et al., 2004). The critical roles of IL-10 in SCI is its reduction of the secondary inflammation (Thompson et al., 2013) leading to improved recovery including neuropathic pain (Lau et al., 2012; Park et al., 2018; Plunkett et al., 2001). Our recent study in mouse traumatic brain injury model demonstrates that IL-10 is significantly increased in microglia/macrophages in the injured cortex of $NOX2^{-/-}$ mice (Barrett et al., 2017). Here we show that IL-10 expression is increased in the injured spinal cord of WT and $NOX2^{-/-}$ SCI mice, and that this effect is significantly greater in $NOX2^{-/-}$ animals. Importantly, our qPCR analysis shows that IL-10 expression is approximately 50%

higher in CD11b+ microglia/macrophages isolated from injured spinal cord tissue of NOX2$^{-/-}$ SCI mice than that in WT SCI mice. Thus, in the absence of NOX2, there is increased IL-10 signaling, which in turn results in enhanced anti-inflammatory microglial/macrophage activation.

Another important finding in this study is that we identify NOX2 regulation for miR-155 level. MiR-155 has been widely studied in inflammation, and its published potent pro-inflammatory actions across immune cell types are unparalleled by any other miRNAs (Gaudet et al., 2017). SCI triggers robust upregulation of miR-155 expression and its deletion reduces inflammation and post-injury tissue damage (Gaudet et al., 2016). In the present study, we demonstrate that SCI-mediated elevation of miR-155 expression is significantly lower in NOX2$^{-/-}$ animals than that in WT mice, and this effect is confirmed in CD11b^{+} microglia/macrophages isolated from injured spinal cord tissue. Moreover, studies show that miR-155 expression doubles in response to LPS in IL-10-deficient cells, demonstrating that endogenous IL-10 can feed back on the system to keep miR-155 expression in check, highlighting an additional mechanism of IL-10 control on the pro-inflammatory response (McCoy et al., 2010). Therefore, we speculate that NOX2 depletion-mediated miR-155 reduction after SCI may result from increased IL-10 signaling, with reduced inflammation and improved recovery in NOX2$^{-/-}$ mice.

The limitation of post-injury pain sensitivity assessed in the present study relates to use of stimulus-evoked pain-like behaviors. However, understanding cortical mechanisms and the modulation of pain processing by NOX2 may be more effectively addressed using non-reflexive methods. Multiple outcome measures should be included in the future investigation, such as Place Escape Avoidance Paradigm (PEAP) and Conditioned Place Preference (CPP) that incorporate the motivational and affective aspects of pain relief (Gregory et al., 2013; Tappe-Theodor and Kuner, 2014). The dose of NOX2ds-tat applied in the present study was based on reported therapeutic effects in mice (Abais et al., 2013; Kumar et al., 2016). Further optimization of drug concentration, therapeutic window, as well as the route of administration will be needed. Gender-related differences after SCI have been reported with regard to neurologic changes and post-traumatic neuropathic pain (Chan et al., 2013; Datto et al., 2015; Farooque et al., 2006; Sipski et al., 2004). Inhibition of NOX2 by apocynin, a non-specific NADPH oxidase inhibitor, improves locomotor functional recovery in middle-aged female mice after SCI (Zhang et al., 2018). However, NOX2-related sex differences have not been reported in CNS injury. Whether or not NOX2$^{-/-}$ female mice recover better than those in male animals after SCI is intriguing for next investigation.

In conclusion, we provide evidence that inhibiting or deleting NOX2 significantly improve long-term locomotor function and limit mechanical/thermal cutaneous hypersensitivity after SCI. Loss of NOX2 in NOX2$^{-/-}$ mice reduces infiltrating macrophages and ROS production, leading to reduced neurotoxic M1-like pro-inflammatory phenotype and to elevated M2-like activation after SCI. Furthermore, depletion of NOX2 promotes IL-10 expression, likely contributing to reduced pro-inflammatory miR-155 level. Together, we attribute improved functional recovery to the ability of NOX2 inhibition to drive an anti-inflammatory response in the injured tissue that is likely mediated by IL-10/miR155 signaling.

Acknowledgements

We thank Drs. Dianer Yang and Lin Zou, Ms. Laina Yu and Shuxin Zhao for expert technical support. This study was supported by the National Institutes of Health Grants 2R01 NR013601 (JW/AIF), R01 NS094527 (JW), and Craig H. Neilsen Foundation senior grant 340442 (AIF). AK was partially supported by the Ramalingaswami Fellowship (BT/RLF/Re-entry/13/2014) from Department of Biotechnology, Ministry of Science and Technology, India

References

Abais JM, Zhang C, Xia M, Liu Q, Gehr TW, Boini KM, Li PL, 2013 NADPH oxidase-mediated triggering of inflammasome activation in mouse podocytes and glomeruli during hyperhomocysteinemia. Antioxidants & redox signaling 18, 1537–1548. [PubMed: 23088210]

Abraham KE, McMillen D, Brewer KL, 2004 The effects of endogenous interleukin-10 on gray matter damage and the development of pain behaviors following excitotoxic spinal cord injury in the mouse. Neuroscience 124, 945–952. [PubMed: 15026134]

Barrett JP, Henry RJ, Villapol S, Stoica BA, Kumar A, Burns MP, Faden AI, Loane DJ, 2017 NOX2 deficiency alters macrophage phenotype through an IL-10/STAT3 dependent mechanism: implications for traumatic brain injury. J Neuroinflammation 14, 65. [PubMed: 28340575]

Basso DM, Fisher LC, Anderson AJ, Jakeman LB, McTigue DM, Popovich PG, 2006 Basso Mouse Scale for locomotion detects differences in recovery after spinal cord injury in five common mouse strains. J Neurotrauma 23, 635–659. [PubMed: 16689667]

Bermudez S, Khayrullina G, Zhao Y, Byrnes KR, 2016 NADPH oxidase isoform expression is temporally regulated and may contribute to microglial/macrophage polarization after spinal cord injury. Mol Cell Neurosci 77, 53–64. [PubMed: 27729244]

Byrnes KR, Washington PM, Knoblach SM, Hoffman E, Faden AI, 2011 Delayed inflammatory mRNA and protein expression after spinal cord injury. J Neuroinflammation 8, 130. [PubMed: 21975064]

Chan WM, Mohammed Y, Lee I, Pearse DD, 2013 Effect of gender on recovery after spinal cord injury. Translational stroke research 4, 447–461. [PubMed: 24323341]

Chen H, Kim GS, Okami N, Narasimhan P, Chan PH, 2011 NADPH oxidase is involved in post-ischemic brain inflammation. Neurobiol Dis 42, 341–348. [PubMed: 21303700]

Chen H, Song YS, Chan PH, 2009 Inhibition of NADPH oxidase is neuroprotective after ischemiareperfusion. J Cereb Blood Flow Metab 29, 1262–1272. [PubMed: 19417757]

Chhaya SJ, Quiros-Molina D, Tamashiro-Orrego AD, Houle JD, Detloff MR, 2018 Exercise-Induced Changes to the Macrophage Response in the Dorsal Root Ganglia Prevent Neuropathic Pain after Spinal Cord Injury. J Neurotrauma.

Choi BY, Kim JH, Kho AR, Kim IY, Lee SH, Lee BE, Choi E, Sohn M, Stevenson M, Chung TN, Kauppinen TM, Suh SW, 2015 Inhibition of NADPH oxidase activation reduces EAE-induced white matter damage in mice. J Neuroinflammation 12, 104. [PubMed: 26017142]

Choi SH, Aid S, Kim HW, Jackson SH, Bosetti F, 2012 Inhibition of NADPH oxidase promotes alternative and anti-inflammatory microglial activation during neuroinflammation. J Neurochem 120, 292–301. [PubMed: 22050439]

Cooney SJ, Zhao Y, Byrnes KR, 2014 Characterization of the expression and inflammatory activity of NADPH oxidase after spinal cord injury. Free radical research 48, 929–939. [PubMed: 24866054]

Datto JP, Bastidas JC, Miller NL, Shah AK, Arheart KL, Marcillo AE, Dietrich WD, Pearse DD, 2015 Female Rats Demonstrate Improved Locomotor Recovery and Greater Preservation of White and Gray Matter after Traumatic Spinal Cord Injury Compared to Males. J Neurotrauma 32, 1146–1157. [PubMed: 25715192]

David S, Kroner A, 2011 Repertoire of microglial and macrophage responses after spinal cord injury. Nat Rev Neurosci 12, 388–399. [PubMed: 21673720]

Detloff MR, Fisher LC, McGaughy V, Longbrake EE, Popovich PG, Basso DM, 2008 Remote activation of microglia and pro-inflammatory cytokines predict the onset and severity of below-level neuropathic pain after spinal cord injury in rats. Exp Neurol 212, 337–347. [PubMed: 18511041]

Farooque M, Suo Z, Arnold PM, Wulser MJ, Chou CT, Vancura RW, Fowler S, Festoff BW, 2006 Gender-related differences in recovery of locomotor function after spinal cord injury in mice. Spinal cord 44, 182–187. [PubMed: 16130019]

Gao X, Kim HK, Chung JM, Chung K, 2007 Reactive oxygen species (ROS) are involved in enhancement of NMDA-receptor phosphorylation in animal models of pain. Pain 131, 262–271. [PubMed: 17317010]

Gaudet AD, Fonken LK, Watkins LR, Nelson RJ, Popovich PG, 2017 MicroRNAs: Roles in Regulating Neuroinflammation. The Neuroscientist : a review journal bringing neurobiology, neurology and psychiatry, 1073858417721150.

Gaudet AD, Mandrekar-Colucci S, Hall JC, Sweet DR, Schmitt PJ, Xu X, Guan Z, Mo X, Gueraude-Arellano M, Popovich PG, 2016 miR-155 Deletion in Mice Overcomes Neuron-Intrinsic and Neuron-Extrinsic Barriers to Spinal Cord Repair. J Neurosci 36, 8516–8532. [PubMed: 27511021]

Gensel JC, Zhang B, 2015 Macrophage activation and its role in repair and pathology after spinal cord injury. Brain Res 1619, 1–11. [PubMed: 25578260]

Gordon S, 2003 Alternative activation of macrophages. Nature reviews. Immunology 3, 23–35.

Gregory NS, Harris AL, Robinson CR, Dougherty PM, Fuchs PN, Sluka KA, 2013 An overview of animal models of pain: disease models and outcome measures. The journal of pain : official journal of the American Pain Society 14, 1255–1269. [PubMed: 24035349]

Gwak YS, Kang J, Unabia GC, Hulsebosch CE, 2012 Spatial and temporal activation of spinal glial cells: role of gliopathy in central neuropathic pain following spinal cord injury in rats. Exp Neurol 234, 362–372. [PubMed: 22036747]

Hansen CN, Fisher LC, Deibert RJ, Jakeman LB, Zhang H, Noble-Haeusslein L, White S, Basso DM, 2013 Elevated MMP-9 in the lumbar cord early after thoracic spinal cord injury impedes motor relearning in mice. J Neurosci 33, 13101–13111. [PubMed: 23926264]

Hassler SN, Johnson KM, Hulsebosch CE, 2014 Reactive oxygen species and lipid peroxidation inhibitors reduce mechanical sensitivity in a chronic neuropathic pain model of spinal cord injury in rats. J Neurochem 131, 413–417. [PubMed: 25051888]

Henry RJ, Doran SJ, Barrett JP, Meadows VE, Sabirzhanov B, Stoica BA, Loane DJ, Faden AI, 2018 Inhibition of miR-155 Limits Neuroinflammation and Improves Functional Recovery After Experimental Traumatic Brain Injury in Mice. Neurotherapeutics.

Holt LM, Olsen ML, 2016 Novel Applications of Magnetic Cell Sorting to Analyze Cell-Type Specific Gene and Protein Expression in the Central Nervous System. PLoS One 11, e0150290. [PubMed: 26919701]

Hulsebosch CE, 2008 Gliopathy ensures persistent inflammation and chronic pain after spinal cord injury. Exp Neurol 214, 6–9. [PubMed: 18708053]

Hulsebosch CE, Hains BC, Crown ED, Carlton SM, 2009 Mechanisms of chronic central neuropathic pain after spinal cord injury. Brain research reviews 60, 202–213. [PubMed: 19154757]

Im YB, Jee MK, Choi JI, Cho HT, Kwon OH, Kang SK, 2012 Molecular targeting of NOX4 for neuropathic pain after traumatic injury of the spinal cord. Cell death & disease 3, e426. [PubMed: 23152062]

Jablonski KA, Amici SA, Webb LM, Ruiz-Rosado Jde D, Popovich PG, Partida-Sanchez S, Gueraude-Arellano M, 2015 Novel Markers to Delineate Murine M1 and M2 Macrophages. PLoS One 10, e0145342. [PubMed: 26699615]

Johnstone JT, Morton PD, Jayakumar AR, Johnstone AL, Gao H, Bracchi-Ricard V, Pearse DD, Norenberg MD, Bethea JR, 2013 Inhibition of NADPH oxidase activation in oligodendrocytes reduces cytotoxicity following trauma. PLoS One 8, e80975. [PubMed: 24260524]

Kallenborn-Gerhardt W, Hohmann SW, Syhr KM, Schroder K, Sisignano M, Weigert A, Lorenz JE, Lu R, Brune B, Brandes RP, Geisslinger G, Schmidtko A, 2014 Nox2-dependent signaling between macrophages and sensory neurons contributes to neuropathic pain hypersensitivity. Pain 155, 2161–2170. [PubMed: 25139590]

Khayrullina G, Bermudez S, Byrnes KR, 2015 Inhibition of NOX2 reduces locomotor impairment, inflammation, and oxidative stress after spinal cord injury. J Neuroinflammation 12, 172. [PubMed: 26377802]

Kigerl KA, Gensel JC, Ankeny DP, Alexander JK, Donnelly DJ, Popovich PG, 2009 Identification of two distinct macrophage subsets with divergent effects causing either neurotoxicity or regeneration in the injured mouse spinal cord. J Neurosci 29, 13435–13444. [PubMed: 19864556]

Kim D, You B, Jo EK, Han SK, Simon MI, Lee SJ, 2010 NADPH oxidase 2-derived reactive oxygen species in spinal cord microglia contribute to peripheral nerve injury-induced neuropathic pain. Proc Natl Acad Sci USA 107, 14851–14856. [PubMed: 20679217]

Kim HK, Park SK, Zhou JL, Taglialatela G, Chung K, Coggeshall RE, Chung JM, 2004 Reactive oxygen species (ROS) play an important role in a rat model of neuropathic pain. Pain 111, 116–124. [PubMed: 15327815]

Kumar A, Alvarez-Croda DM, Stoica BA, Faden AI, Loane DJ, 2015 Microglial/Macrophage Polarization Dynamics following Traumatic Brain Injury. J Neurotrauma.

Kumar A, Barrett JP, Alvarez-Croda DM, Stoica BA, Faden AI, Loane DJ, 2016 NOX2 drives M1-like microglial/macrophage activation and neurodegeneration following experimental traumatic brain injury. Brain Behav Immun.

Lambeth JD, 2004 NOX enzymes and the biology of reactive oxygen. Nature reviews. Immunology 4, 181–189.

Lau D, Harte SE, Morrow TJ, Wang S, Mata M, Fink DJ, 2012 Herpes simplex virus vector-mediated expression of interleukin-10 reduces below-level central neuropathic pain after spinal cord injury. Neurorehabilitation and neural repair 26, 889–897. [PubMed: 22593113]

Little JW, Doyle T, Salvemini D, 2012 Reactive nitroxidative species and nociceptive processing: determining the roles for nitric oxide, superoxide, and peroxynitrite in pain. Amino Acids 42, 75–94. [PubMed: 20552384]

Liu S, Sarkar C, Dinizo M, Faden AI, Koh EY, Lipinski MM, Wu J, 2015 Disrupted autophagy after spinal cord injury is associated with ER stress and neuronal cell death. Cell death & disease 6, e1582. [PubMed: 25569099]

Liu W, Chen Q, Liu J, Liu KJ, 2011 Normobaric hyperoxia protects the blood brain barrier through inhibiting Nox2 containing NADPH oxidase in ischemic stroke. Med Gas Res 1, 22. [PubMed: 22146586]

Loane DJ, Byrnes KR, 2010 Role of microglia in neurotrauma. Neurotherapeutics 7, 366–377. [PubMed: 20880501]

Loane DJ, Kumar A, Stoica BA, Cabatbat R, Faden AI, 2014 Progressive neurodegeneration after experimental brain trauma: association with chronic microglial activation. J Neuropathol Exp Neurol 73, 14–29. [PubMed: 24335533]

Loane DJ, Stoica BA, Byrnes KR, Jeong W, Faden AI, 2013 Activation of mGluR5 and inhibition of NADPH oxidase improves functional recovery after traumatic brain injury. Journal of neurotrauma 30, 403–412. [PubMed: 23199080]

Loane DJ, Stoica BA, Pajoohesh-Ganji A, Byrnes KR, Faden AI, 2009 Activation of metabotropic glutamate receptor 5 modulates microglial reactivity and neurotoxicity by inhibiting NADPH oxidase. J Biol Chem 284, 15629–15639. [PubMed: 19364772]

Lu R, Kallenborn-Gerhardt W, Geisslinger G, Schmidtko A, 2011 Additive antinociceptive effects of a combination of vitamin C and vitamin E after peripheral nerve injury. PLoS One 6, e29240. [PubMed: 22195029]

Lynch MA, 2009 The multifaceted profile of activated microglia. Molecular neurobiology 40, 139–156. [PubMed: 19629762]

Matyas JJ, O'Driscoll CM, Yu L, Coll-Miro M, Daugherty S, Renn CL, Faden AI, Dorsey SG, Wu J, 2017 Truncated TrkB.T1-Mediated Astrocyte Dysfunction Contributes to Impaired Motor Function and Neuropathic Pain after Spinal Cord Injury. J Neurosci 37, 3956–3971. [PubMed: 28270575]

McCoy CE, Sheedy FJ, Qualls JE, Doyle SL, Quinn SR, Murray PJ, O'Neill LA, 2010 IL-10 inhibits miR-155 induction by toll-like receptors. J Biol Chem 285, 20492–20498. [PubMed: 20435894]

Mukhamedshina YO, Akhmetzyanova ER, Martynova EV, Khaiboullina SF, Galieva LR, Rizvanov AA, 2017 Systemic and Local Cytokine Profile following Spinal Cord Injury in Rats: A Multiplex Analysis. Frontiers in neurology 8, 581. [PubMed: 29163344]

Norden DM, Faw TD, McKim DB, Deibert RJ, Fisher LC, Sheridan JF, Godbout JP, Basso Dm Ed.D P.T., 2018 Bone Marrow-derived Monocytes Drive the Inflammatory Microenvironment in Local and Remote Regions after Thoracic SCI. J Neurotrauma.

Park J, Decker JT, Smith DR, Cummings BJ, Anderson AJ, Shea LD, 2018 Reducing inflammation through delivery of lentivirus encoding for anti-inflammatory cytokines attenuates neuropathic pain after spinal cord injury. J Control Release 290, 88–101. [PubMed: 30296461]

Peng XM, Zhou ZG, Glorioso JC, Fink DJ, Mata M, 2006 Tumor necrosis factor-alpha contributes to below-level neuropathic pain after spinal cord injury. Ann Neurol 59, 843–851. [PubMed: 16634039]

Plunkett JA, Yu CG, Easton JM, Bethea JR, Yezierski RP, 2001 Effects of interleukin-10 (IL-10) on pain behavior and gene expression following excitotoxic spinal cord injury in the rat. Exp Neurol 168, 144–154. [PubMed: 11170729]

Qin H, Holdbrooks AT, Liu Y, Reynolds SL, Yanagisawa LL, Benveniste EN, 2012 SOCS3 deficiency promotes M1 macrophage polarization and inflammation. Journal of immunology 189, 3439–3448.

Ren K, Dubner R, 1999 Central nervous system plasticity and persistent pain. J Orofac Pain 13, 155–163; discussion 164-171. [PubMed: 10823030]

Ritter DM, Zemel BM, Hala TJ, O'Leary ME, Lepore AC, Covarrubias M, 2015 Dysregulation of Kv3.4 channels in dorsal root ganglia following spinal cord injury. J Neurosci 35, 1260–1273. [PubMed: 25609640]

Sabirzhanov B, Stoica BA, Zhao Z, Loane DJ, Wu J, Dorsey SG, Faden AI, 2016 miR-711 upregulation induces neuronal cell death after traumatic brain injury. Cell Death Differ 23, 654–668. [PubMed: 26470728]

Sabirzhanov B, Zhao Z, Stoica BA, Loane DJ, Wu J, Borroto C, Dorsey SG, Faden AI, 2014 Downregulation of miR-23a and miR-27a following experimental traumatic brain injury induces neuronal cell death through activation of proapoptotic Bcl-2 proteins. J Neurosci 34, 10055–10071. [PubMed: 25057207]

Salvemini D, Little JW, Doyle T, Neumann WL, 2011 Roles of reactive oxygen and nitrogen species in pain. Free Radic Biol Med 51, 951–966. [PubMed: 21277369]

Schwab ME, Bartholdi D, 1996 Degeneration and regeneration of axons in the lesioned spinal cord. Physiological reviews 76, 319–370. [PubMed: 8618960]

Seo JE, Hasan M, Rahaman KA, Kang MJ, Jung BH, Kwon OS, 2016 A leading role for NADPH oxidase in an in-vitro study of experimental autoimmune encephalomyelitis. Mol Immunol 72, 19–27. [PubMed: 26928315]

Siddall PJ, McClelland JM, Rutkowski SB, Cousins MJ, 2003 A longitudinal study of the prevalence and characteristics of pain in the first 5 years following spinal cord injury. Pain 103, 249–257. [PubMed: 12791431]

Siniscalco D, Fuccio C, Giordano C, Ferraraccio F, Palazzo E, Luongo L, Rossi F, Roth KA, Maione S, de Novellis V, 2007 Role of reactive oxygen species and spinal cord apoptotic genes in the development of neuropathic pain. Pharmacol Res 55, 158–166. [PubMed: 17207636]

Sipski ML, Jackson AB, Gomez-Marin O, Estores I, Stein A, 2004 Effects of gender on neurologic and functional recovery after spinal cord injury. Archives of physical medicine and rehabilitation 85, 1826–1836. [PubMed: 15520978]

Stormer S, Gerner HJ, Gruninger W, Metzmacher K, Follinger S, Wienke C, Aldinger W, Walker N, Zimmermann M, Paeslack V, 1997 Chronic pain/dysaesthesiae in spinal cord injury patients: results of a multicentre study. Spinal cord 35, 446–455. [PubMed: 9232750]

Tappe-Theodor A, Kuner R, 2014 Studying ongoing and spontaneous pain in rodents--challenges and opportunities. Eur J Neurosci 39, 1881–1890. [PubMed: 24888508]

Thompson CD, Zurko JC, Hanna BF, Hellenbrand DJ, Hanna A, 2013 The therapeutic role of interleukin-10 after spinal cord injury. J Neurotrauma 30, 1311–1324. [PubMed: 23731227]

Vargas ME, Barres BA, 2007 Why is Wallerian degeneration in the CNS so slow? Annual review of neuroscience 30, 153–179.

von Leden RE, Yauger YJ, Khayrullina G, Byrnes KR, 2016 Central Nervous System Injury and Nicotinamide Adenine Dinucleotide Phosphate Oxidase: Oxidative Stress and Therapeutic Targets. J Neurotrauma.

Walters ET, 2014 Neuroinflammatory contributions to pain after SCI: roles for central glial mechanisms and nociceptor-mediated host defense. Exp Neurol 258, 48–61. [PubMed: 25017887]

Wu J, Renn CL, Faden AI, Dorsey SG, 2013 TrkB.T1 contributes to neuropathic pain after spinal cord injury through regulation of cell cycle pathways. J Neurosci 33, 12447–12463. [PubMed: 23884949]

Wu J, Sabirzhanov B, Stoica BA, Lipinski MM, Zhao Z, Zhao S, Ward N, Yang D, Faden AI, 2015 Ablation of the transcription factors E2F1–2 limits neuroinflammation and associated neurological deficits after contusive spinal cord injury. Cell Cycle 14, 3698–3712. [PubMed: 26505089]

Wu J, Yoo S, Wilcock D, Lytle JM, Leung PY, Colton CA, Wrathall JR, 2010 Interaction of NG2(+) glial progenitors and microglia/macrophages from the injured spinal cord. Glia 58, 410–422. [PubMed: 19780197]

Wu J, Zhao Z, Kumar A, Lipinski MM, Loane DJ, Stoica BA, Faden AI, 2016a Endoplasmic Reticulum Stress and Disrupted Neurogenesis in the Brain Are Associated with Cognitive Impairment and Depressive-Like Behavior after Spinal Cord Injury. J Neurotrauma.

Wu J, Zhao Z, Sabirzhanov B, Stoica BA, Kumar A, Luo T, Skovira J, Faden AI, 2014 Spinal cord injury causes brain inflammation associated with cognitive and affective changes: role of cell cycle pathways. J Neurosci 34, 10989–11006. [PubMed: 25122899]

Wu J, Zhao Z, Zhu X, Renn CL, Dorsey SG, Faden AI, 2016b Cell cycle inhibition limits development and maintenance of neuropathic pain following spinal cord injury. Pain 157, 488–503. [PubMed: 26797506]

Wu JF, Stoica BA, Dinizo M, Pajoohesh-Ganji A, Piao CS, Faden AI, 2012 Delayed cell cycle pathway modulation facilitates recovery after spinal cord injury. Cell Cycle 11, 1782–1795. [PubMed: 22510563]

Zhang B, Bailey WM, McVicar AL, Gensel JC, 2016 Age increases reactive oxygen species production in macrophages and potentiates oxidative damage after spinal cord injury. Neurobiol Aging 47, 157–167. [PubMed: 27596335]

Zhang B, Bailey WM, McVicar AL, Stewart AN, Veldhorst AK, Gensel JC, 2018 Reducing age-dependent monocyte-derived macrophage activation contributes to the therapeutic efficacy of NADPH oxidase inhibition in spinal cord injury. Brain Behav Immun.

Zhang QG, Laird MD, Han D, Nguyen K, Scott E, Dong Y, Dhandapani KM, Brann DW, 2012 Critical role of NADPH oxidase in neuronal oxidative damage and microglia activation following traumatic brain injury. PLoS One 7, e34504. [PubMed: 22485176]

Zhou D, Chen L, Yang K, Jiang H, Xu W, Luan J, 2017 SOCS molecules: the growing players in macrophage polarization and function. Oncotarget 8, 60710–60722. [PubMed: 28948005]

Highlights

- Inhibition of NOX2 alleviates post-SCI pain-related behavior and motor dysfunction
- NOX2 deficiency alters microglial/macrophage activation
- $NOX2^{-/-}$ reduces $CD11b^{+}/CD45^{hi}/F4/80^{+}$ macrophage infiltration and ROS production
- NOX2 deficiency limits inflammation, possibly by modulating IL-10/miR-155 signaling

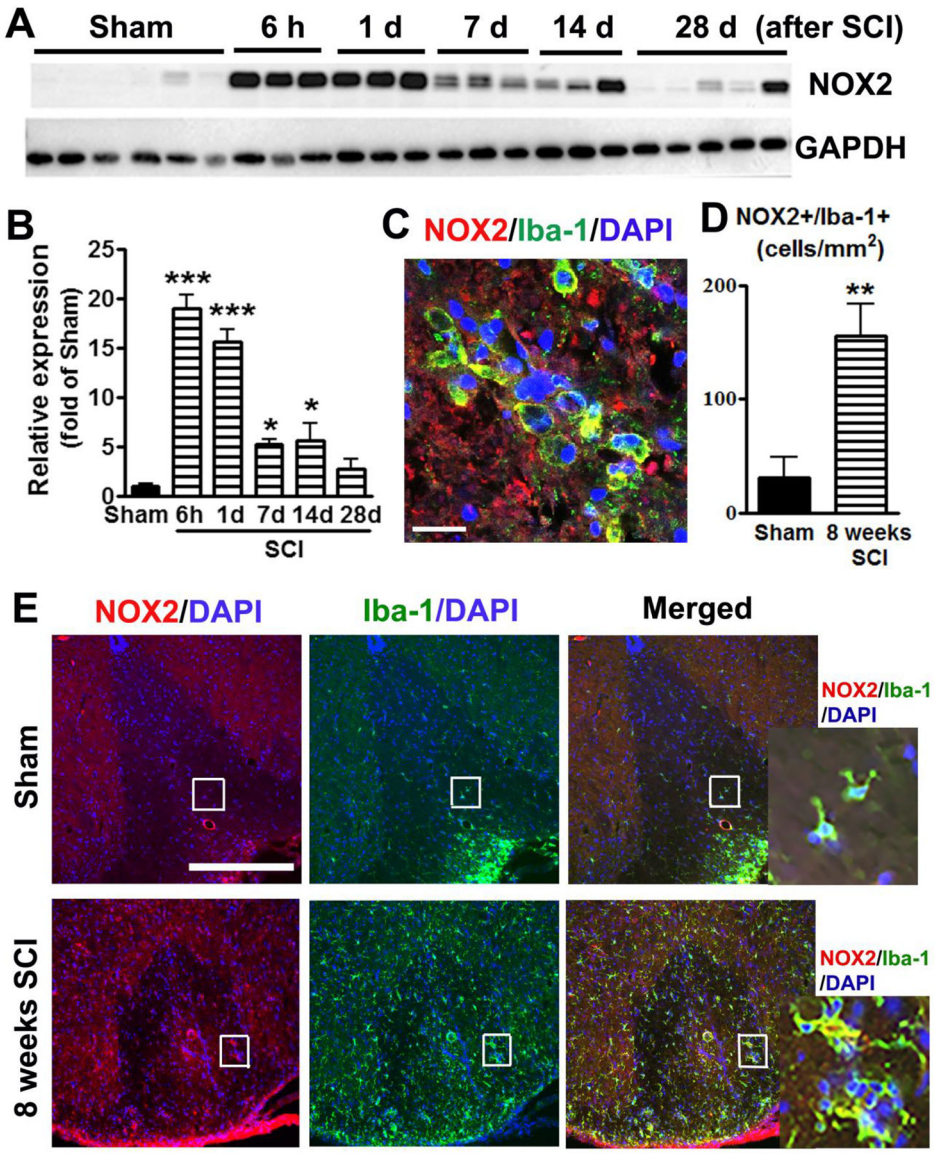

Figure 1.

SCI induces upregulation of NOX2 expression predominantly in microglia/macrophages. (A-B) NOX2 elevation in injured spinal cord tissue. n=3–6 mice/group. *p<0.05, ***p<0.001 vs Sham. (C) At 24h after SCI, NOX2 expression by Iba-1+ microglia/ macrophages at the lesion core. Scale bar = 25 μm. (D) $NOX2^{+}$/$Iba\text{-}1^{+}$ cells are significantly increased (3 fold) at the lesion site from 8 weeks SCI mice. N=5 mice/group. **p<0.01 vs Sham. (E) Representative images for $NOX2^{+}$/$Iba\text{-}1^{+}$ cells in the dorsal white matter at 0.2 mm rostral to the epicenter from Sham and 8 weeks SCI mice. Scale bar = 50 μm. Insets display high magnification images.

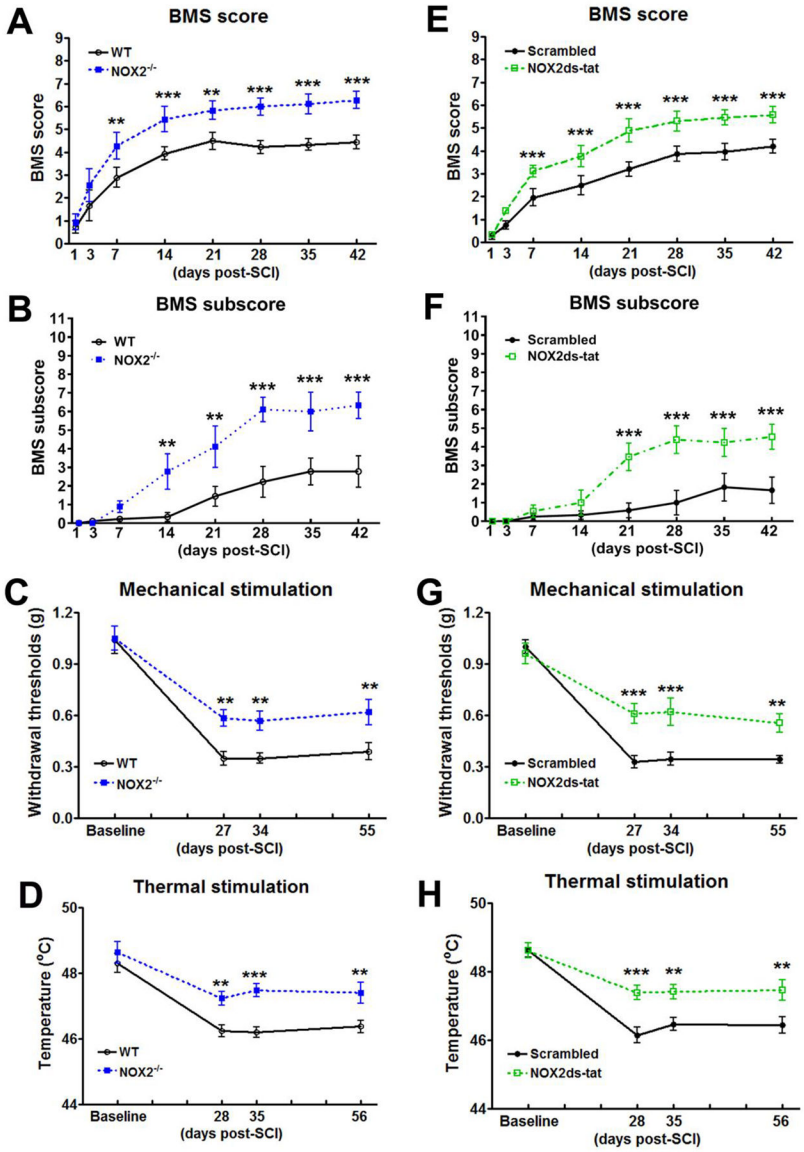

Figure 2.

NOX2 ablation or inhibition improves motor functional recovery and limits cutaneous hypersensitivity after SCI. (A-D) Genetic deletion of NOX2 in NOX2$^{-/-}$ mice increases BMS scores (A) and subscore (B), and limits SCI-induced cutaneous hypersensitivity in Von Frey mechanical (C) and thermal (D) stimulations. N=9–14 mice/group. **p<0.01, ***p<0.001 vs WT. (E-H) Inhibition of NOX2 by NOX2 ds-tat tat (5 mg/kg by ip) beginning at 3 hours post-injury and once daily for 7 days increases BMS scores and subscore (E-F) and limits mechanical/thermal cutaneous hypersensitivity (G-H) after SCI. N=7–13 mice/group. **p<0.01, ***p<0.001 vs Scrambled vehicle.

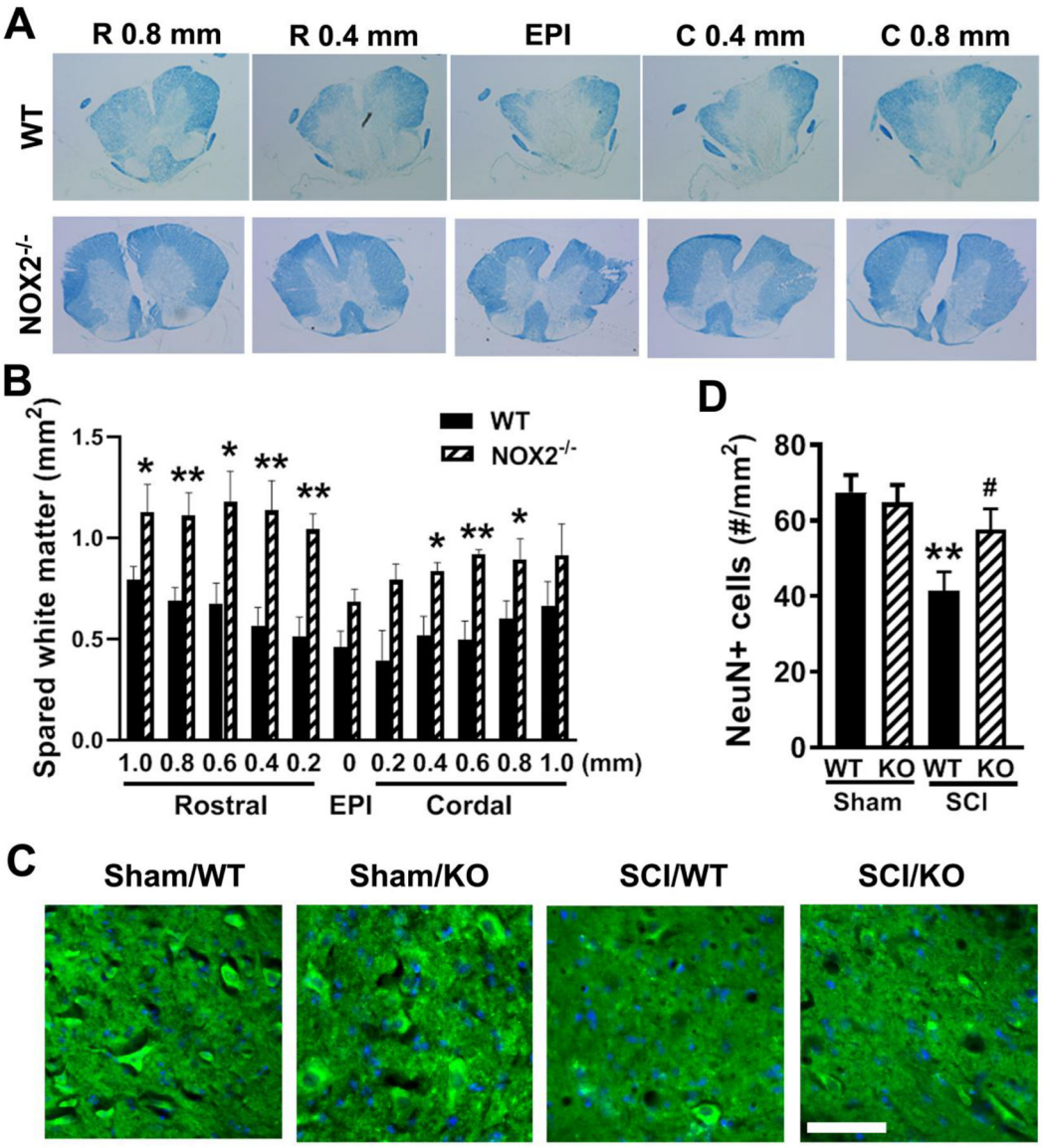

Figure 3.

NOX2 ablation protects against tissue damage induced by SCI. (A-B) Spared whiter matter (SWM) at 8 weeks post-injury was assessed on LFB stained coronal sections. NOX2 deficiency increased spared tissue in the whiter matter at the epicenter (EPI) as well as rostral or cordal to the EPI. Representative images encompassed the rostral (R, 0.8, 0.4 mm) to caudal (C, 0.8, 0.4 mm) extent of the lesion from WT and NOX2$^{-/-}$ group. *p < 0.05, **p < 0.01 vs. WT. (C) Representative images of NeuN^{+} cells (green) in the ventral horns at 0.1 mm rostral to the EPI. (D) Quantification of NeuN^{+} cells showed significantly more neurons survived in the gray matter of the NOX2$^{-/-}$ mice compared to their WT littermates. N=5 (WT) and 6 (NOX2$^{-/-}$) mice. *p < 0.05, ***p < 0.001 vs. WT. Scale bar = 50μm.

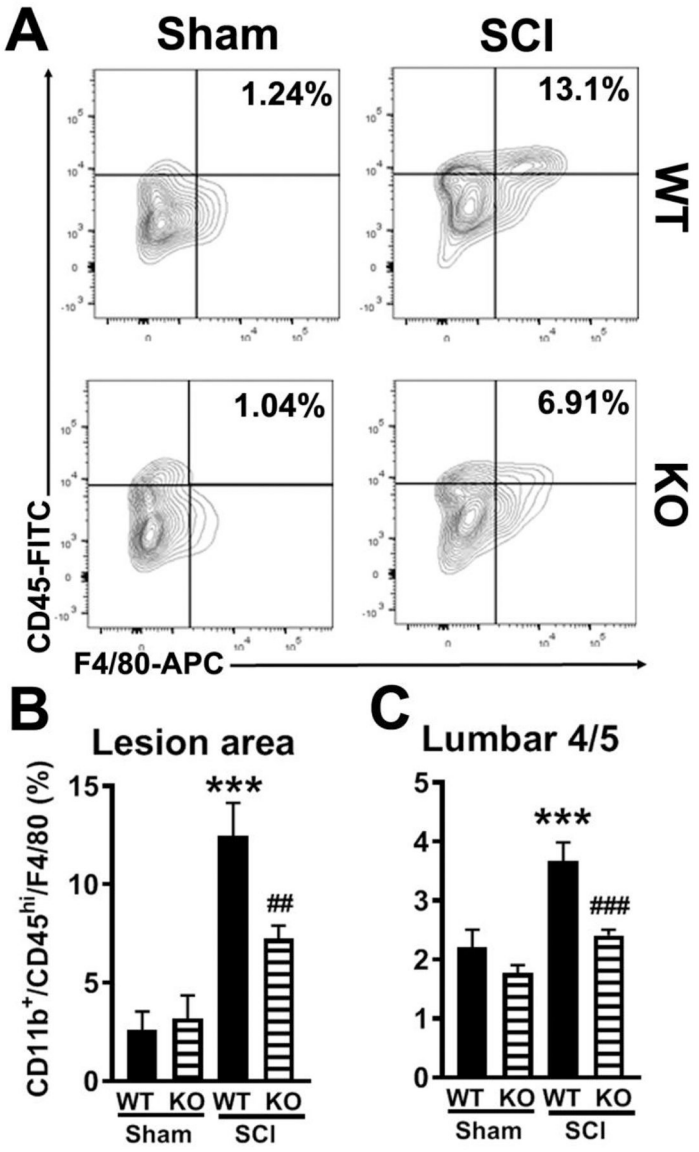

Figure 4.

Depletion of NOX2 reduces macrophage infiltration at 24h after SCI. (A) Representative histogram for $CD11b^{+}CD45^{hi}F4/80^{+}$ cells at the lesion area. (B-C) Flow cytometry analysis of $CD11b^{+}CD45^{hi}F4/80^{+}$ population in the lesion area and lumbar 4/5 cord from WT and $NOX2^{-/-}$ (KO) sham and SCI mice at 1d post-injury. N=5–6 mice/group. ***p<0.001 vs WT/Sham; $^{\#\#}$p<0.01, $^{\#\#\#}$p<0.001 vs WT/SCI.

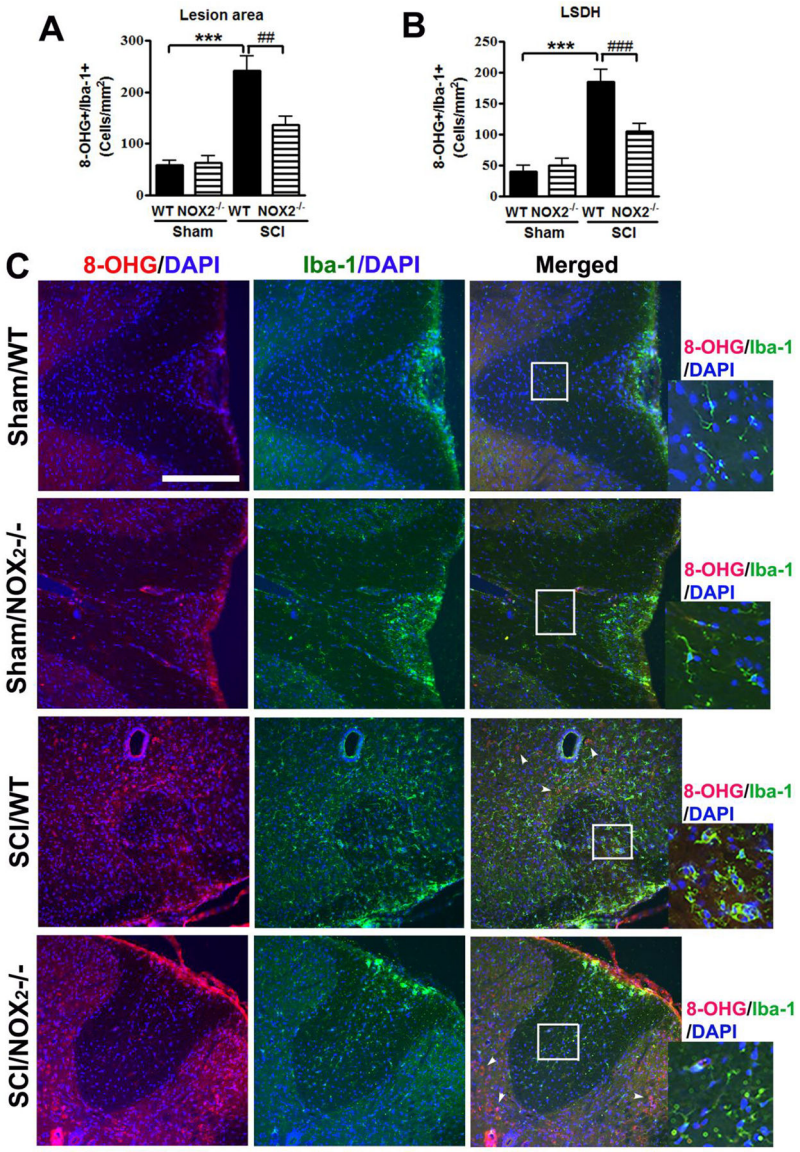

Figure 5.

Deletion of NOX2 reduces ROS production in Iba-1^{+} cells at 8 weeks after SCI. (A-B) 8-OHG^{+}/Iba-1^{+} cells were quantified at the lesion epicenter (A) and the lumbar spinal cord horn (LSDH, B) after SCI. N=7 (Sham/WT), 6 (Sham/NOX2$^{-/-}$), 8 (SCI/WT), and 5 (SCI/NOX2$^{-/-}$) mice/group. ***p<0.001 vs WT/Sham; $^{\#\#}$p<0.01, $^{\#\#\#}$p<0.001 vs WT/SCI. (C) Representative images for 8-OHG^{+} (red)/Iba-1^{+} microglia/macrophage (green) in the dorsal white matter at 0.2 mm rostral to the epicenter. Scale bar = 50 μm. Insets display high magnification images from Sham and NOX2$^{-/-}$ mice. Some of the 8-OHG^{+} cells in the grey matter are Iba-1^{-} (arrowheads) from SCI mice.

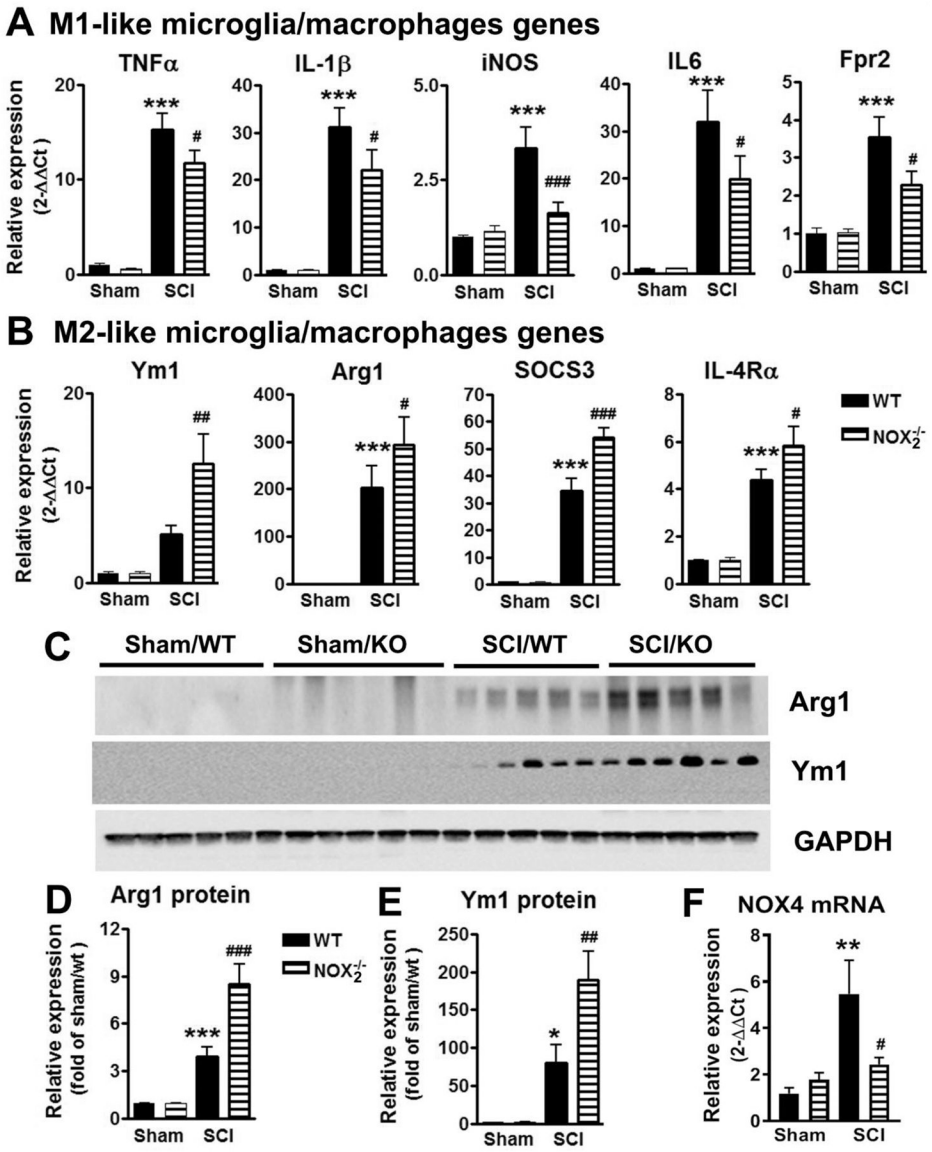

Figure 6.

NOX2 deficiency attenuates M1-like activation (A) and promotes M2-like activation (B) in the injured tissue at 1d post-SCI. N=5–7 mice/group. ***p<0.001 vs WT/Sham; #p<0.05, ##p<0.01, ###p<0.001 vs WT/SCI. (C-E) NOX2 deficiency increases Arginase1 (Arg1) and Ym1 protein expression in the injured spinal cord tissue at 3d post-SCI. (F) NOX2$^{-/-}$ mice displayed significant reduction of NOX4 mRNA at 24h post-injury. N=6 mice/group. **p<0.01 vs WT/Sham; #p<0.05 vs WT/SCI.

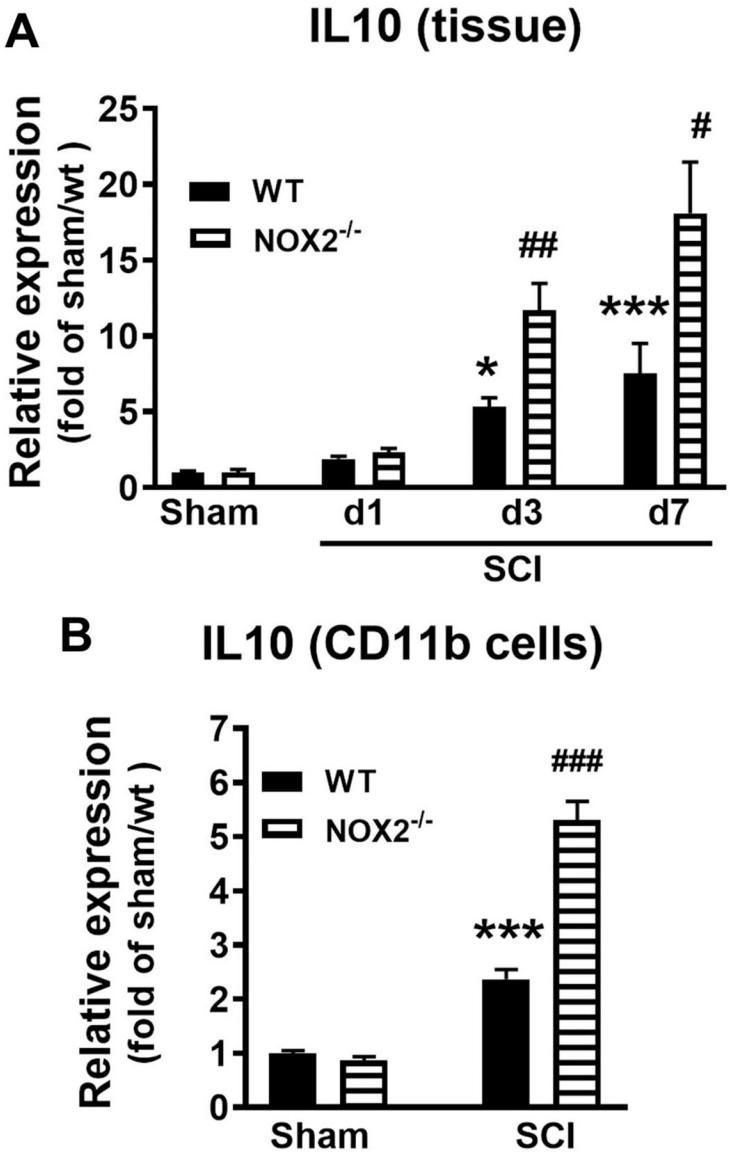

Figure 7.

NOX2 deficiency alters IL-10 expression after SCI. (A) IL-10 mRNA expression was measured in lesion area of sham and SCI WT and NOX2$^{-/-}$ mice at 1, 3, and 7 days post-injury. N=5–6 mice/group. *p<0.05, ***p<0.001 vs Sham/WT; $^{\#}$p<0.05, $^{\#\#}$p<0.01 vs SCI/WT. (B) IL-10 expression in the isolated CD11b+ microglia/macrophage cells derived from 3 days post-injury. N=6 mice/group. ***p<0.001 vs Sham/WT; $^{\#\#\#}$p<0.001 vs SCI/WT.

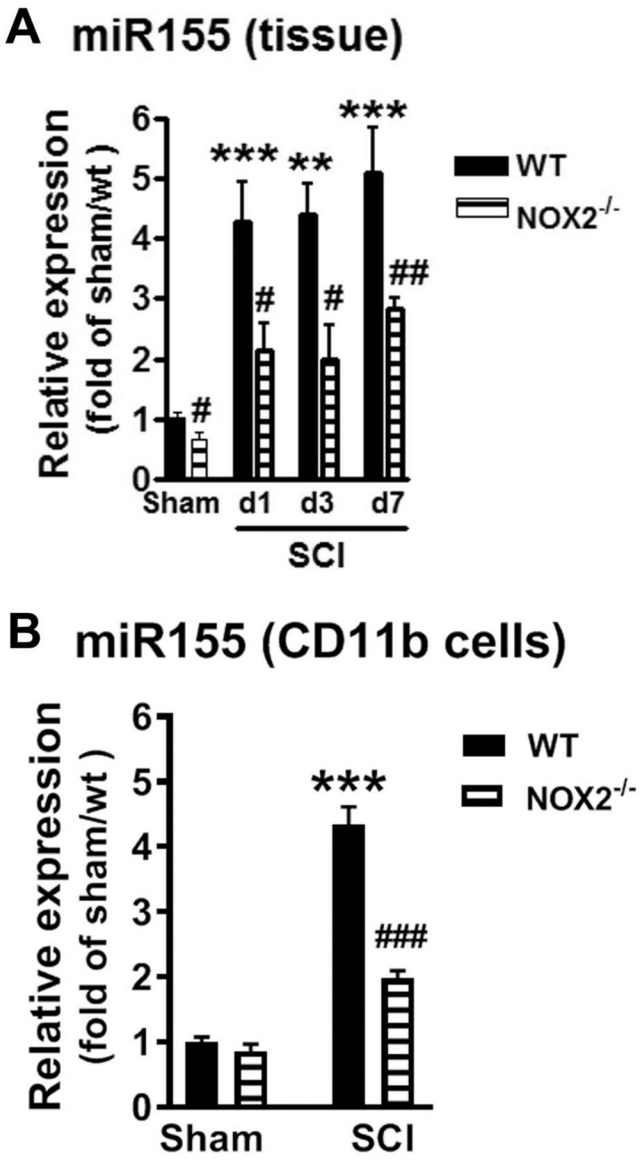

Figure 8.

NOX2 deficiency alters miR-155 expression after SCI. (A) miR-155 expression was measured in lesion area of sham and SCI WT and NOX2$^{-/-}$ mice at 1, 3, and 7 days post-injury. N=5–6 mice/group. **p<0.01, ***p<0.001 vs Sham/WT; $^{\#}$p<0.05, $^{\#\#}$p<0.01 vs SCI/WT. (B) miR-155 expression in the isolated CD11b^{+} microglia/macrophage cells derived from 3 days post-injury. N=9 (Sham/WT), 8 (Sham/NOX2$^{-/-}$), 7 (SCI/WT), and 7 (SCI/NOX2$^{-/-}$) mice/group. ***p<0.001 vs Sham/WT; $^{\#\#\#}$p<0.001 vs SCI/WT.